

Experimental Overview on the QCD Critical Point Search in Heavy-ion Collisions at RHIC

- selected results from RHIC beam energy scan

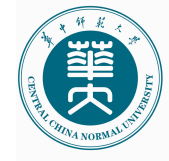


Xiaofeng Luo

Central China Normal University

Oct. 06, 2020

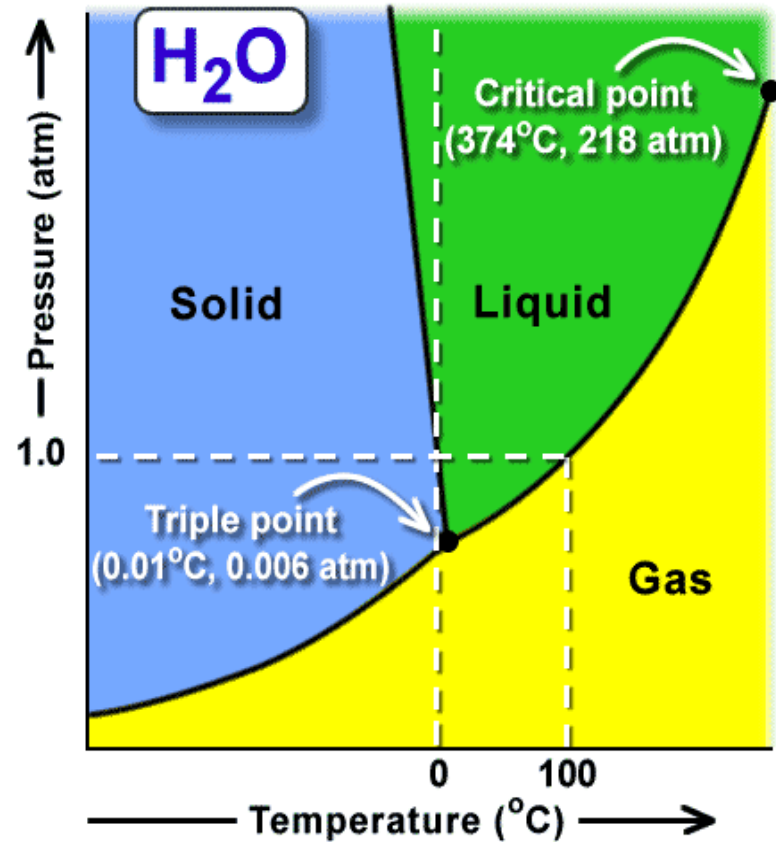




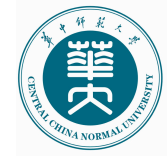
Phase Diagram: Water



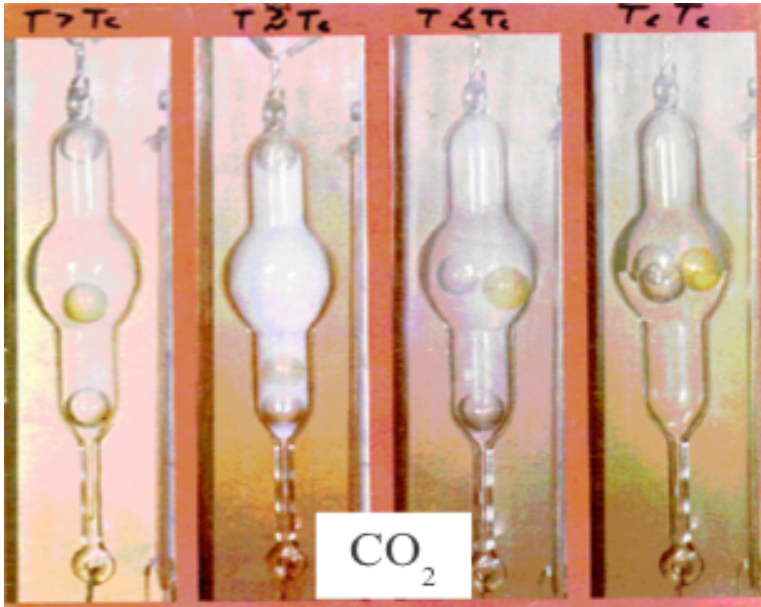
How matter self-organized by varying external conditions.



Thermal motion Vs. Interactions
(Chaos) (Ordered)



Critical Point and Critical Phenomena



- First CP was discovered in 1869 for CO₂ by Andrews.

$$T_c = 31^\circ\text{C}$$

Explained by Van der Waals (1873)
Nobel Prize 1910.

$$\left(P + a \frac{n^2}{V^2}\right) (V - nb) = nRT$$

T. Andrews. Phil. Trans. Royal Soc., 159:575 (1869).

<https://royalsocietypublishing.org/doi/pdf/10.1098/rstl.1869.0021>


Reviewed by : J. C. Maxwell, Nature 10, 477 (1874)

Critical Phenomena :


- Singularity of EoS : divergence of correlation length (ξ), susceptibilities (χ), heat capacity (C_V), critical opalescence.
- Universality and critical exponents : determined by degree of freedom and symmetry of system. (Landau mean field theory, renormalization group theory)
- Finite size effects.




Theory of strong interaction : Quantum Chromodynamics (QCD)

 The Nobel Prize in Physics 2004


"for the discovery of asymptotic freedom in the theory of the strong interaction"



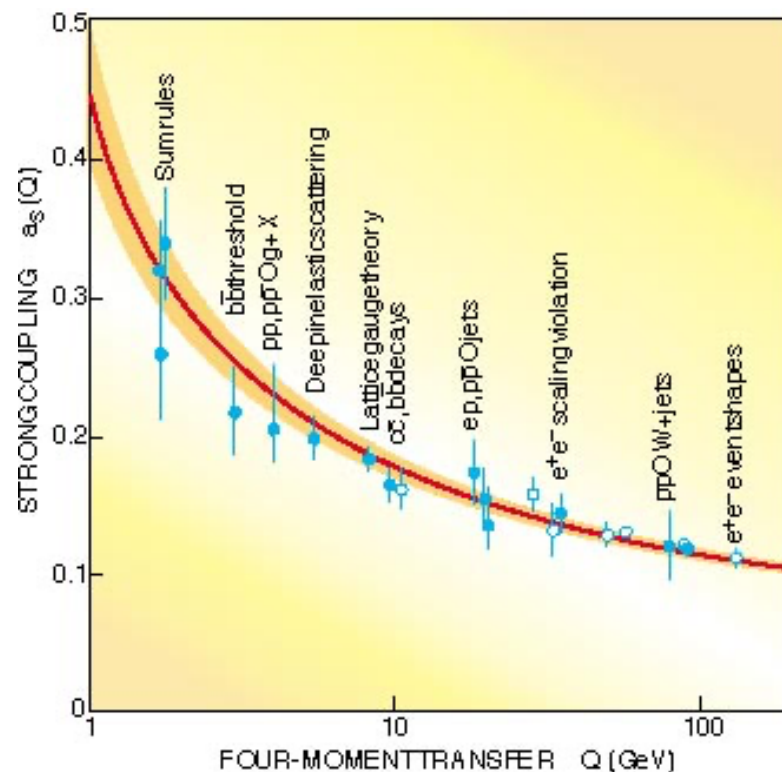
David J. Gross



H. David Politzer



Frank Wilczek



➤ **Asymptotic freedom:** Quarks and Gluons weakly interacting

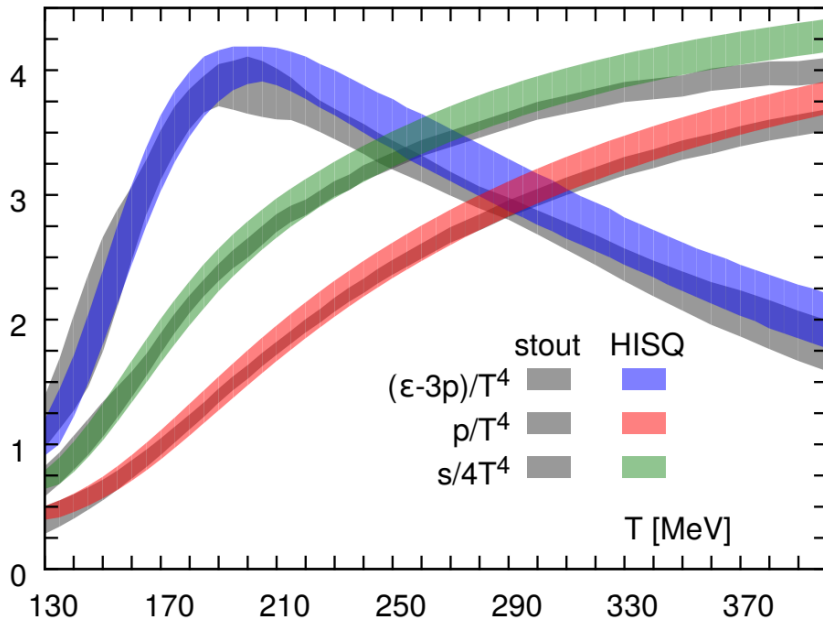
- 1): when close together
- 2): large momentum transfer.

➤ **Confinement:** No free quarks and gluons observed in nature.

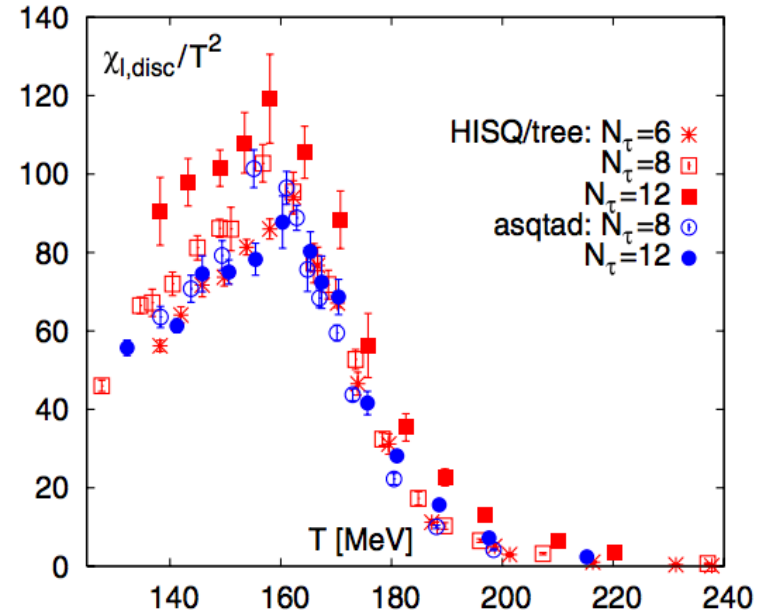
Can we free the quark and gluons from hadrons and create a new form of matter ?



QCD Thermodynamics ($\mu_B=0$) : Lattice QCD



A. Bazavov, et al. (hotQCD), PRD 90, 094503 (2014)



S Borsanyi, et al. (WB), JHEP 1009, 073 (2010).
 T. Bhattacharya, et al (hotQCD), PRL 113, 082001 (2014);
 A. Bazavov *hotQCD*, PRD 85,054503 (2012); PLB 795, 15 (2019)

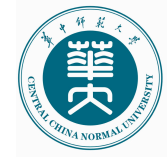
Rapid rise of the energy density:

- Rapid increase in degrees of freedom due to transition from hadrons to quarks and gluons.

Chiral susceptibility peaks at T_c :

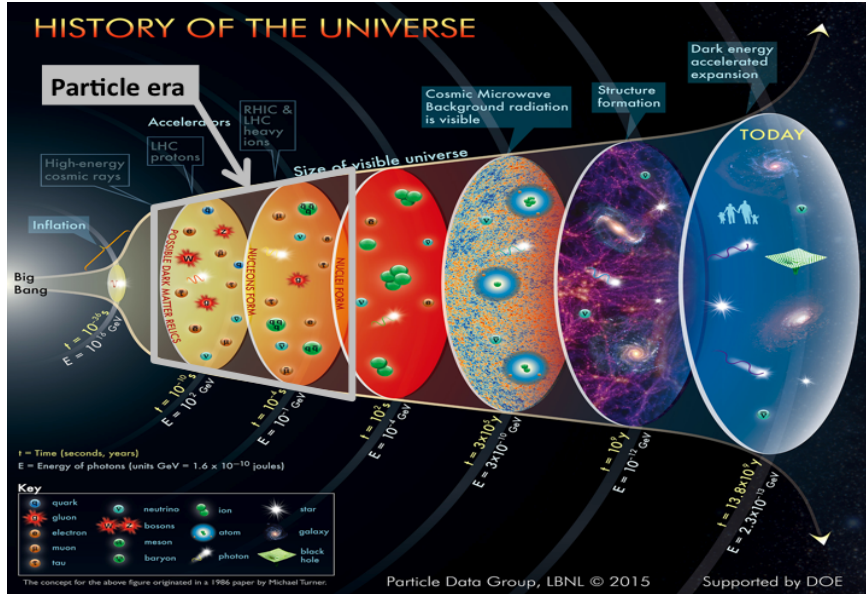
$$\chi_{\bar{\Psi}\Psi} = \frac{T}{V} \frac{\partial^2 \ln Z}{\partial m^2}$$

Transition at $\mu_B=0$ with $T_c \sim 156$ MeV
 \sim trillion $^\circ\text{C}$ (10^{12})

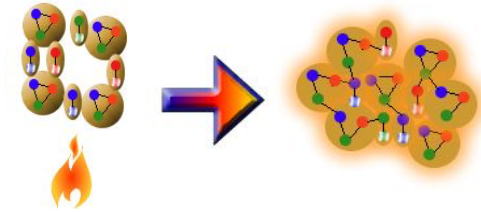


Heat matter to trillion (10^{12}) °C

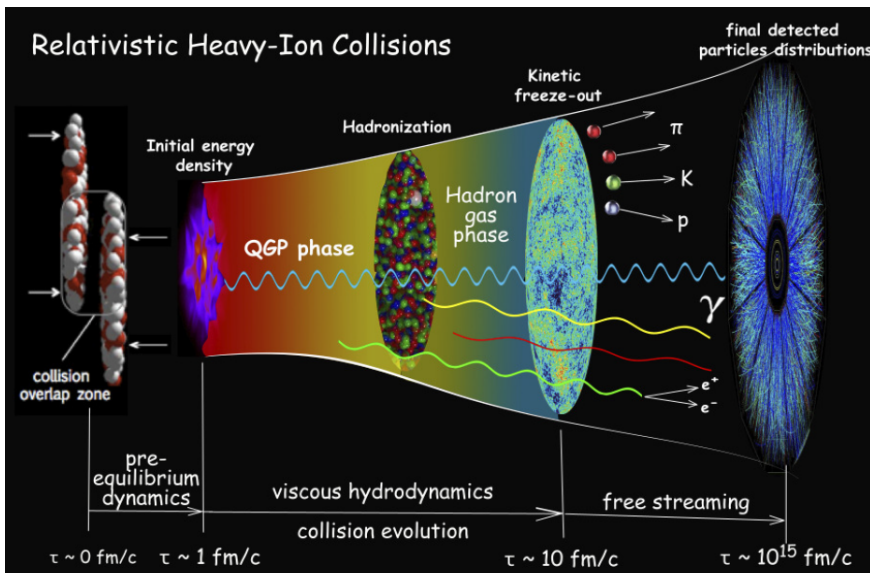
Big Bang



Quark-Gluon Plasma (**QGP**): a state of matter where the quarks and gluons are the relevant degrees of freedom, exist at few μ s after the Big-Bang



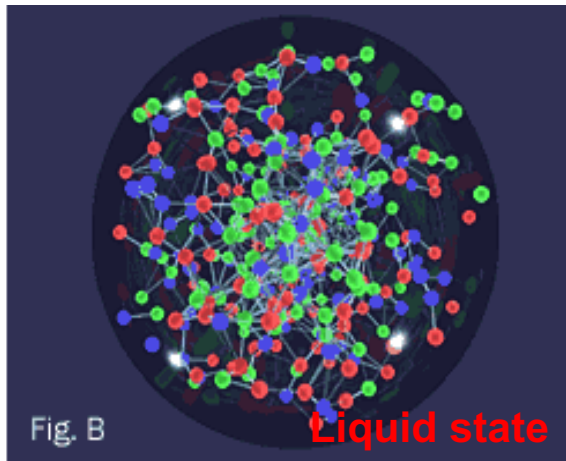
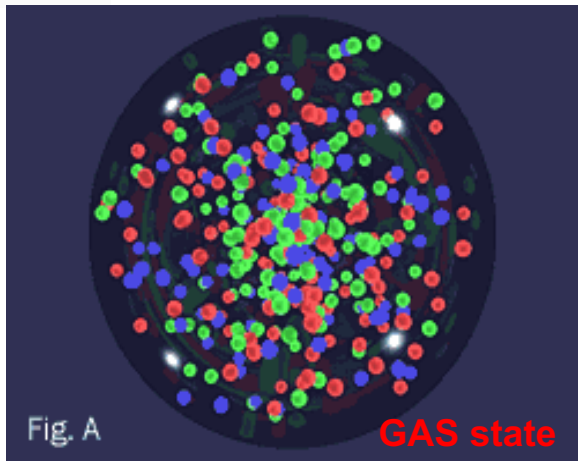
Little Bang



Relativistic heavy-ion collisions are a unique tool to create and study hot QCD matter and its phase transition under controlled conditions

T. D. Lee and G. C. Wick, Phys. Rev. D 9, 2291 (1974). Vacuum stability and vacuum excitation in a spin-0 field theory.

Scientists Serve Up “Perfect” Liquid

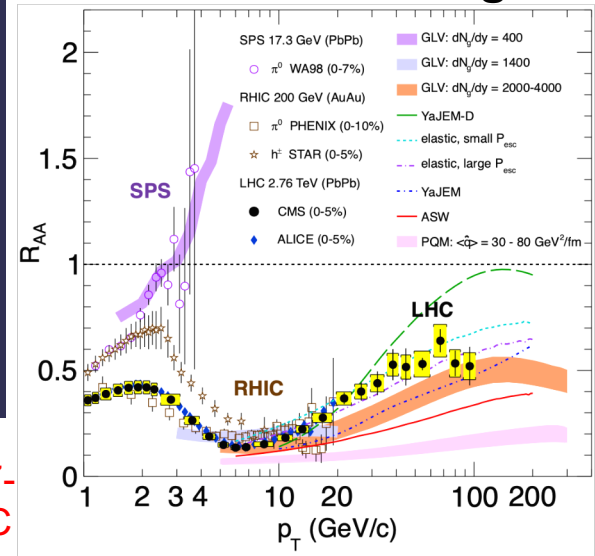


Quark matter studied in nuclear collisions, since 1987 at BNL/AGS (2.7-4.8 GeV), 1996 at CERN/SPS (6.2-17.3 GeV), since 2000 at BNL/RHIC (7.7-200 GeV), since 2010 at the CERN/LHC at $\sqrt{s_{NN}} = 2.76-5.02$ TeV.

Experimental observations support the formation of **strongly couple and liquid like** Quark- Gluon Plasma (sQGP) in Heavy-ion Collisions.

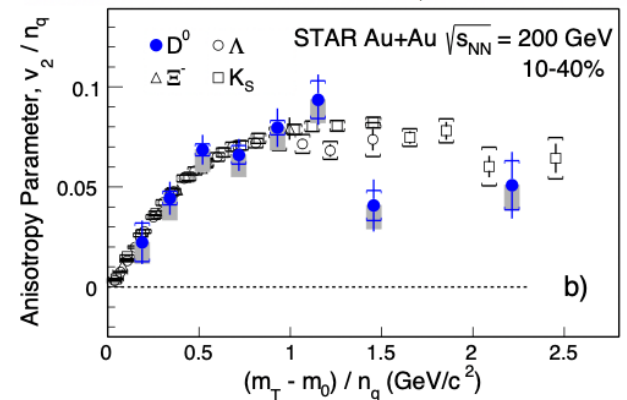
- Low viscosity
- Rapid thermalization
- Jet quenching and medium response
- Partonic collectivity
- Strong electromagnetic field and large vorticity

Jet Quenching



Eur.Phys.J. C72,1945 (2012).

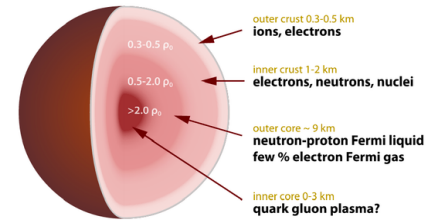
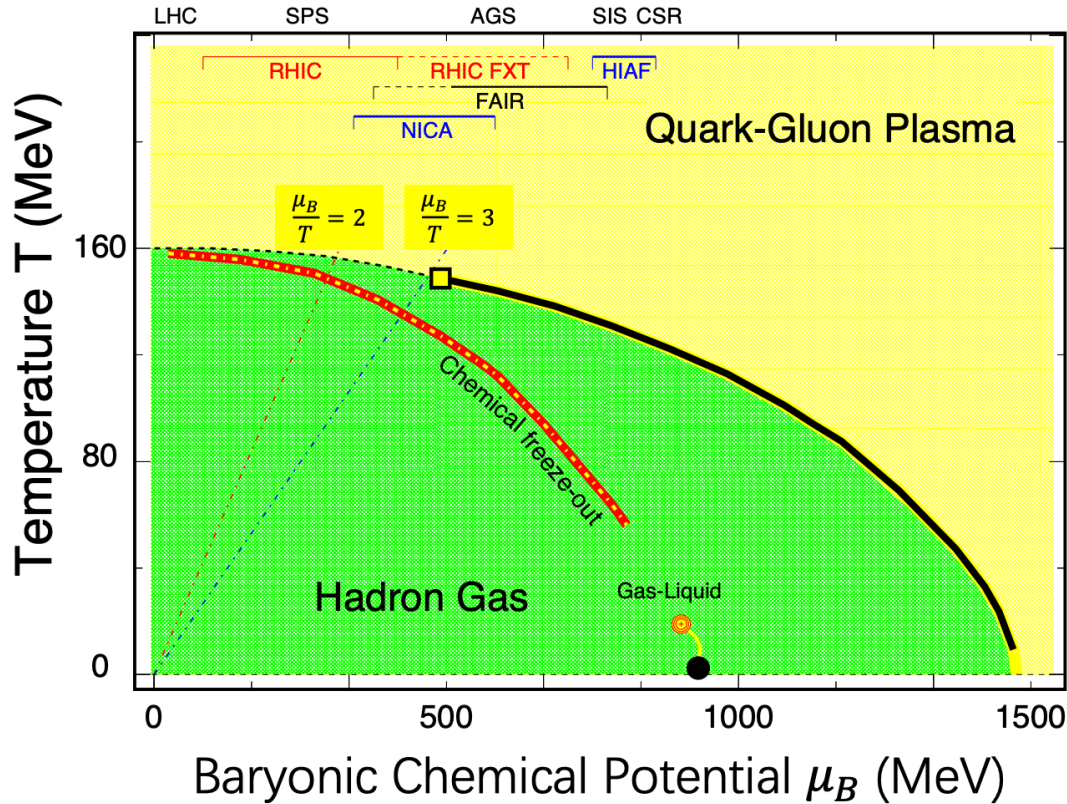
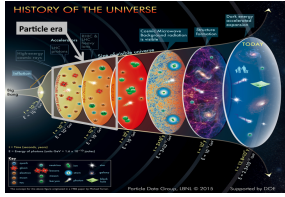
Partonic Collectivity v_2



Phys. Rev. Lett. 117, 212301 (2017).



QCD Phase Diagram



Y. Aoki et al., Nature 443, 675 (2006) ; A. Bazavov et al, PRD 85, 054503 (2012).
 K. Fukushima and C. Sasaki, Prog. Part. Nucl. Phys, 72, 99 (2013).
 A. Bzdak et al., Phys. Rep. 853, 1 (2020).

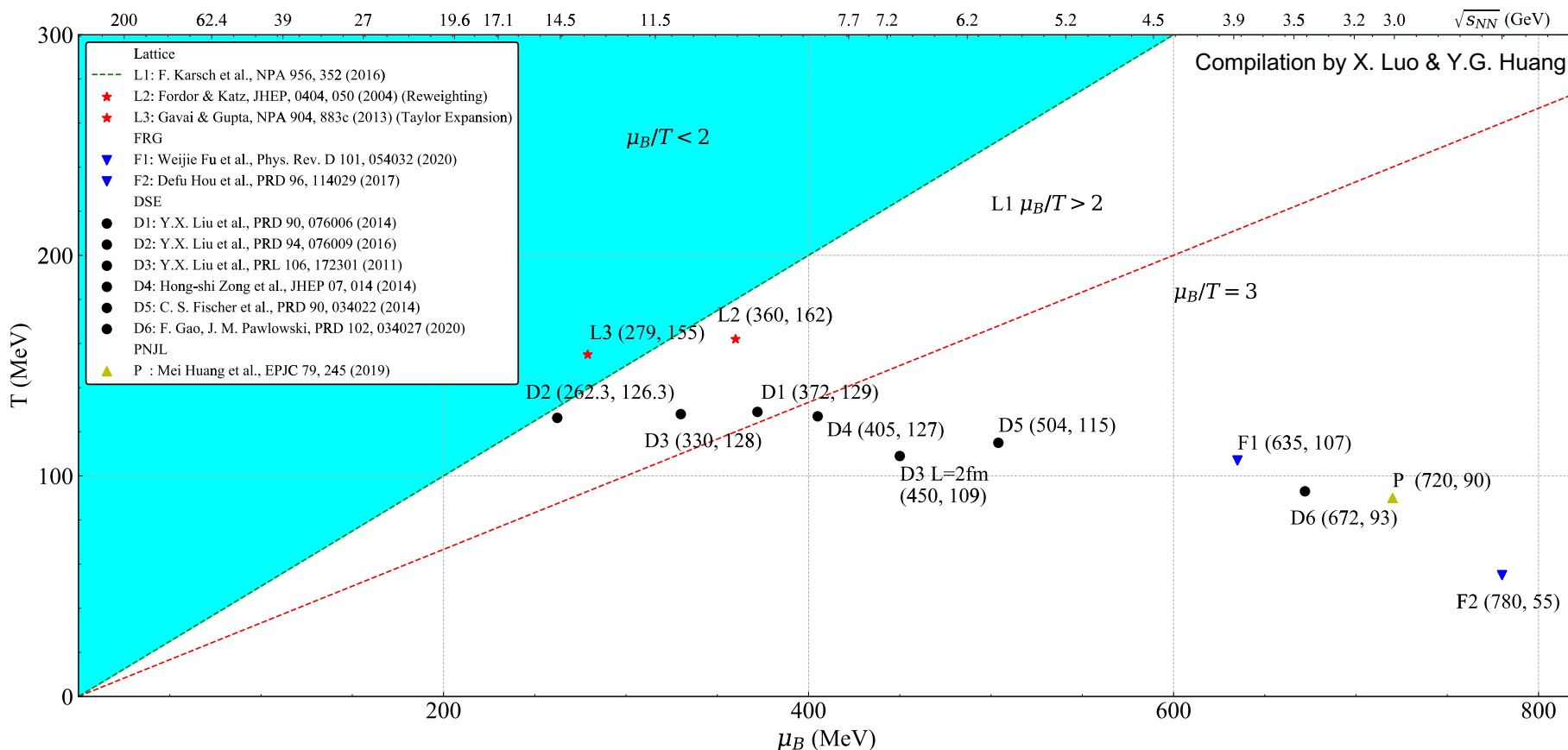
Key question : is there a QCD critical point at finite baryon density region?

Its confirmation will greatly enhance our understanding of the universe evolution and structure of visible matter.



Location of CP : Theoretical Prediction

Preliminary collection from Lattice, DSE, FRG and PNJL (2004-2020)



Large uncertainties for the estimation of CP location.

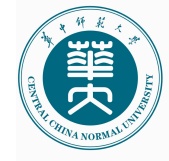


Strategy for the Critical Point Search in HIC

1. Scan the QCD phase diagram and use sensitive experimental observables.
2. Optimize the experimental methods to precisely measure the observables in heavy-ion collisions
3. Dynamical modeling heavy-ion collisions with critical fluctuations.
4. Understanding the experimental and/or physics background (non-CP) and extract the CP signal.

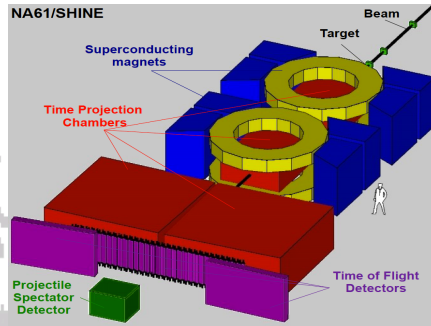
Need collaborative work between experimentalist and theorist

Invited Review : X. Luo and N. Xu, Nucl. Sci. Tech. 28, 112 (2017)



Current and Future Facilities for exploring the QCD Phase Structure

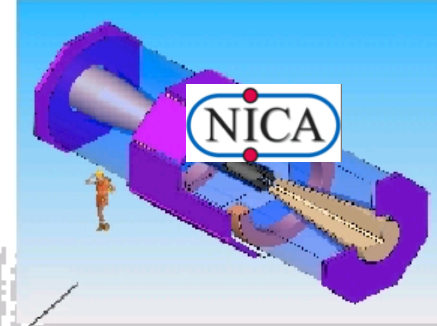
CERN SPS



Fix target

$$\sqrt{s_{NN}} = 5-17 \text{ GeV}$$

Construction....

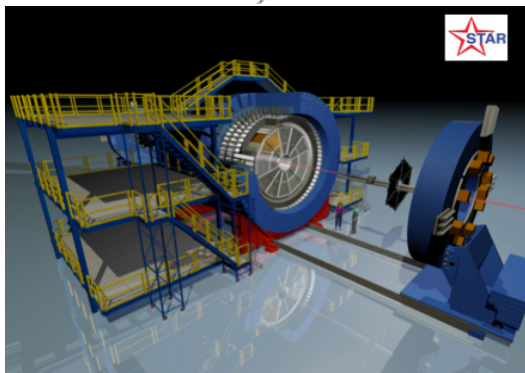


Collider

$$\sqrt{s_{NN}} = 4-11 \text{ GeV (2023-)}$$

BNL/RHIC STAR

BES-I (2010-2017)
BES-II (2018-2021) is ongoing.



Collider $\sqrt{s_{NN}} = 7.7-200 \text{ GeV}$

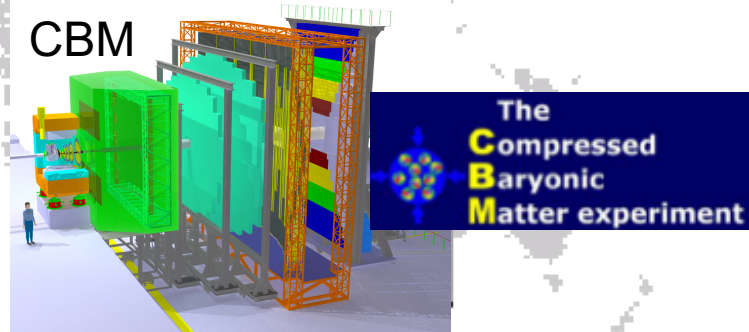
SIS
SPS

NICA

CEE@Lanzhou

JPARC@Japan

Construction....

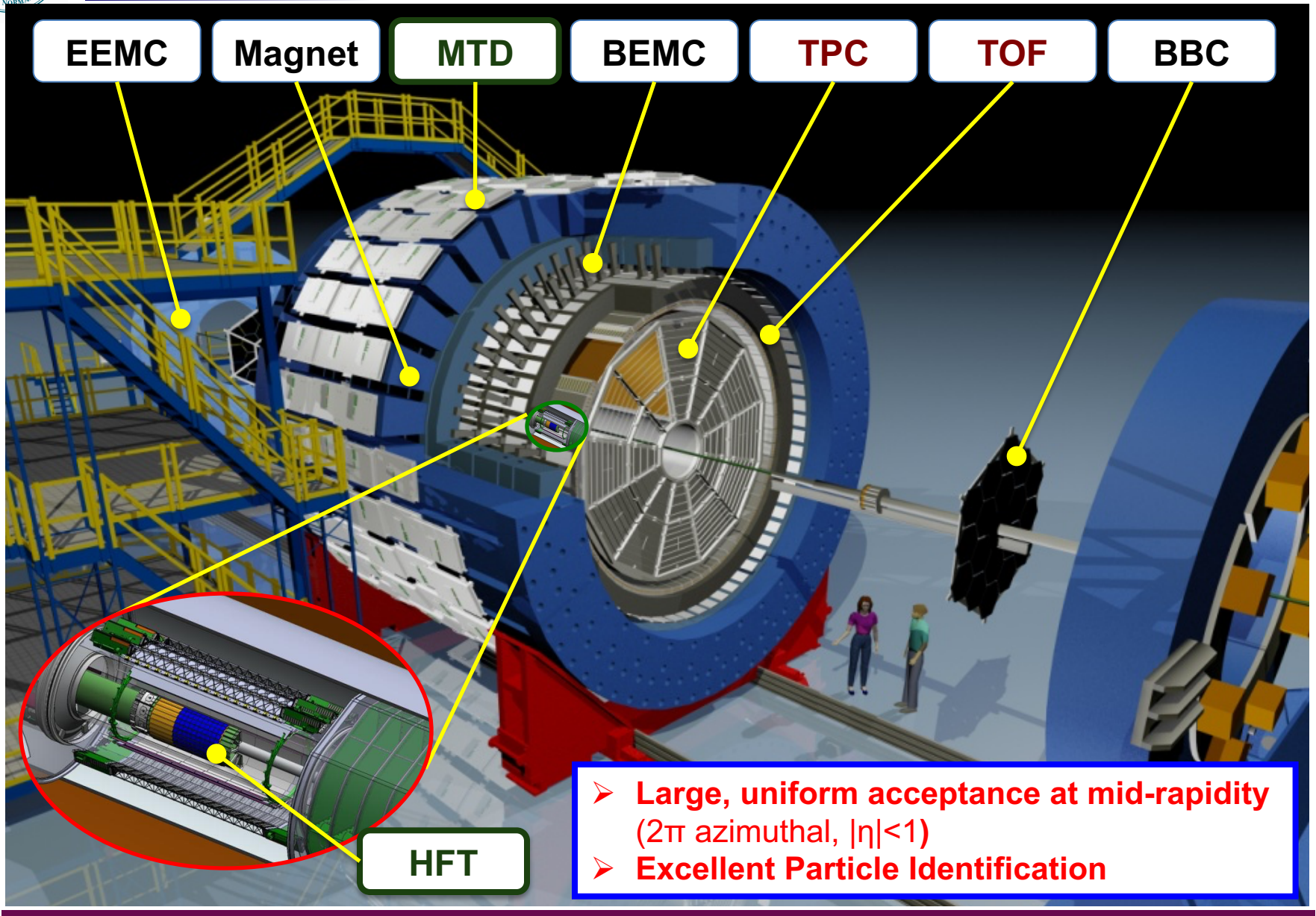


Fix target

$$\sqrt{s_{NN}} = 2-5 \text{ GeV (2025-)}$$



STAR Detector System



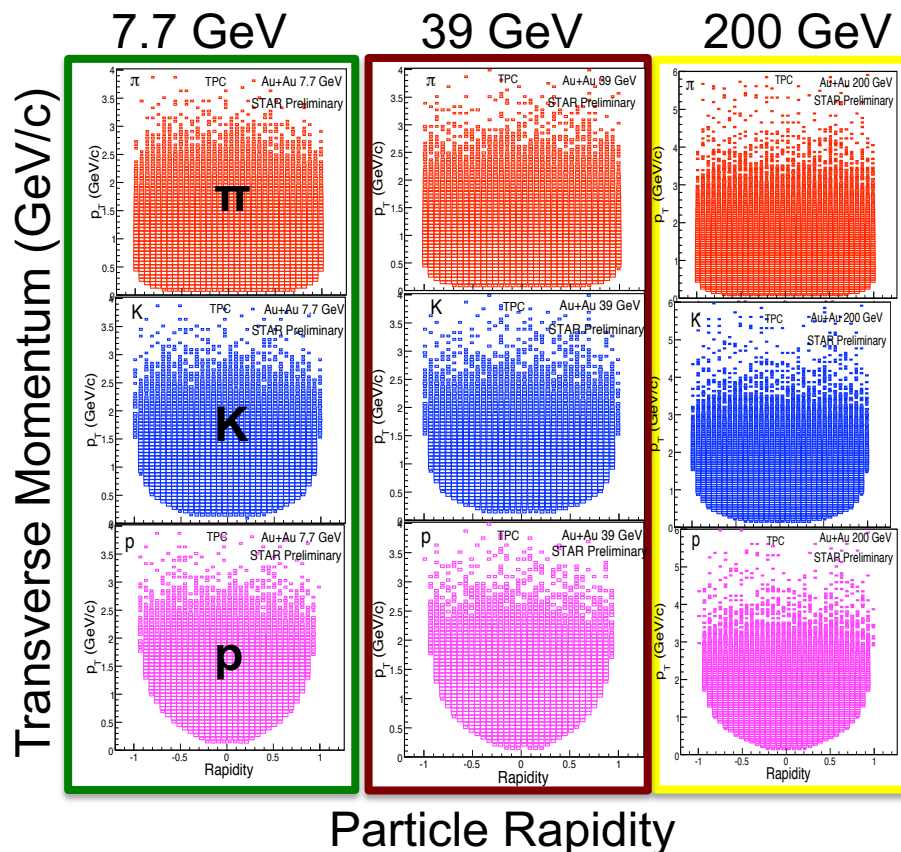


RHIC Beam Energy Scan - I (2010-2017)

Au+Au Collisions

$\sqrt{s_{NN}}$ (GeV)	Events (X10 ⁶)	Year	* μ_B (MeV)	* T_{CH} (MeV)
200	238	2010	25	166
62.4	46	2010	73	165
54.4	1200	2017	83	165
39	86	2010	112	164
27	30	2011	156	162
19.6	15	2011	206	160
14.5	13	2014	264	156
11.5	7	2010	315	152
7.7	3	2010	420	140

Uniform acceptance at Mid-rapidity



*(μ_B , T_{CH}) : J. Cleymans et al., PRC73, 034905 (2006)

STAR, arXiv:1007.2613

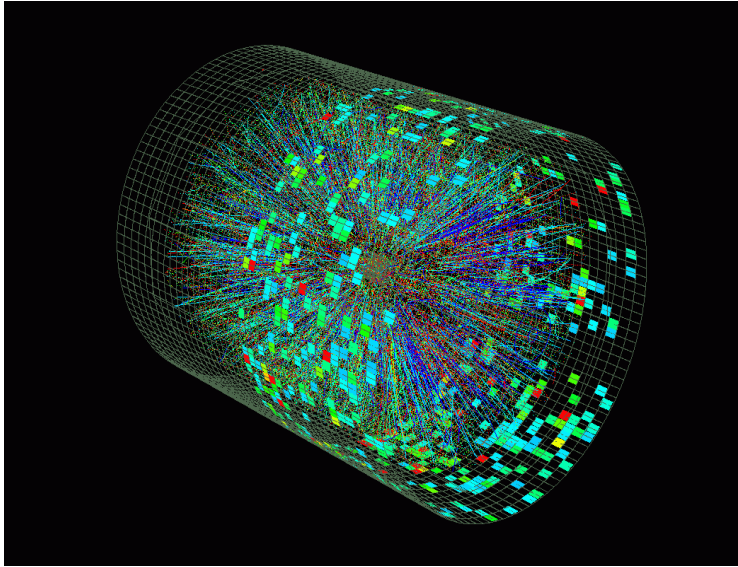
<https://drupal.star.bnl.gov/STAR/starnotes/public/sn0493>

<https://drupal.star.bnl.gov/STAR/starnotes/public/sn0598>

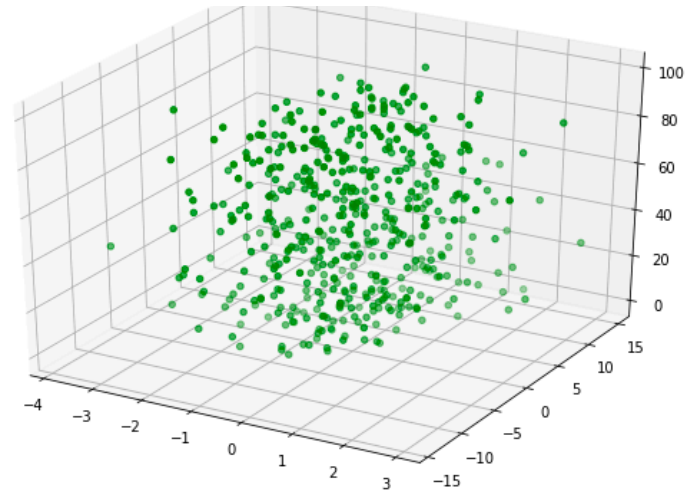
- Access the QCD phase diagram: vary collision energies and/or system size.

RHIC BES-I : 25 < μ_B < 420 MeV

Measurements



$$f(p_{x1}, p_{y1}, p_{z1}, p_{x2}, p_{y2}, p_{z2} \dots)$$



1. Particle Momentum $(p_x, p_y, p_z) \rightarrow (p_T, y, \phi)$
2. Particle Identification (dE/dx, TOF etc.).

Probability Density Distributions in **Momentum Space**

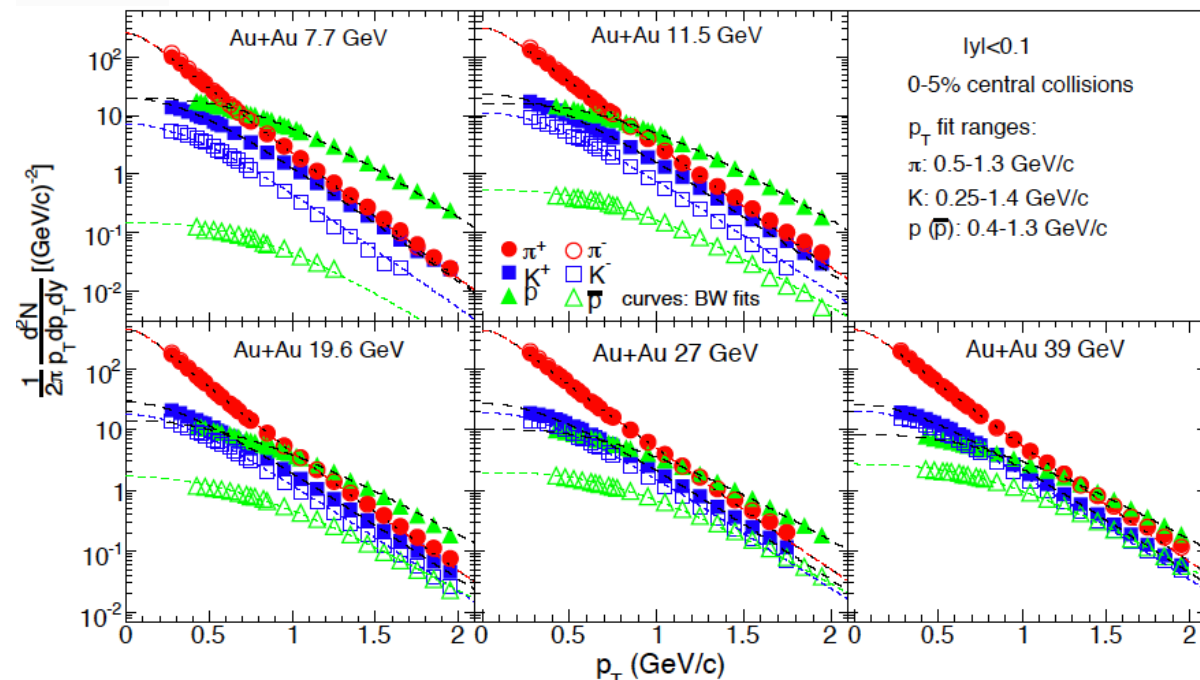
$$\text{Prob.} = f(p_{x1}, p_{y1}, p_{z1}, p_{x2}, p_{y2}, p_{z2}, \dots, p_{xn}, p_{yn}, p_{zn})$$

- Particle multiplicity, p_T spectra, dN/dy etc.
- Multi-particle correlation functions (p_T, y, ϕ , mul.):
differential (HBT, $C_2(\Delta\Phi, \Delta\eta)$, etc.) and integral (flow, cumulants, factorial moments etc.).

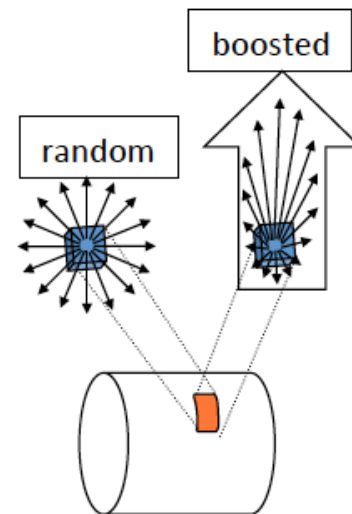
Due to unperfect of detector/methods, various corrections and uncertainties estimation – things that experimentalist spend much time to do.



Kinetic Freeze-out Dynamics : Collective Expansion



Blast Wave Model



STAR: Phys. Rev. C 96, 044904 (2017).

$$E \frac{d^3N}{dp^3} \propto \int_{\sigma} e^{-(u^{\mu} p_{\mu})/T_{fo}} p d\sigma_{\mu} \Rightarrow$$

$$\frac{dN}{m_T dm_T} \propto \int_0^R r dr m_T K_1 \left(\frac{m_T \cosh \rho}{T_{fo}} \right) I_0 \left(\frac{p_T \sinh \rho}{T_{fo}} \right)$$

$$\rho = \tanh^{-1} \beta_T \quad \beta_T = \beta_s \left(\frac{r}{R} \right)^{\alpha} \quad \alpha = 0.5, 1, 2$$

E. Schnedermann, J. Sollfrank, and U. Heinz, PRC 48,2462 (1993).

Expanding source is **assumed** to be:

1. Locally thermal equilibrated.
2. Boosted in radial direction.

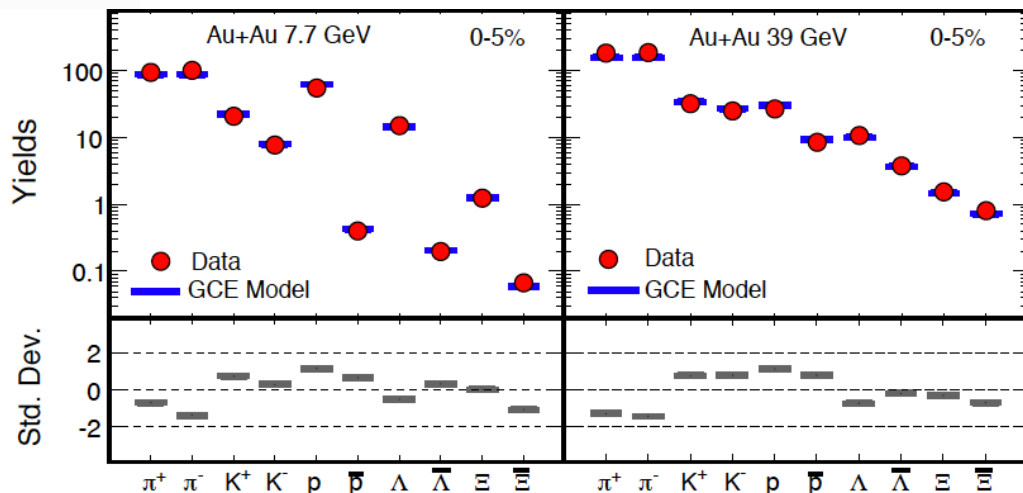
Matters flow with the same velocity.

Fit p_T spectra to obtain parameters:

- Thermal temperature : T_{fo} ,
- Transverse velocity parameter: $\langle \beta_T \rangle$



Chemical Freeze-out : Data Vs. Thermal Model

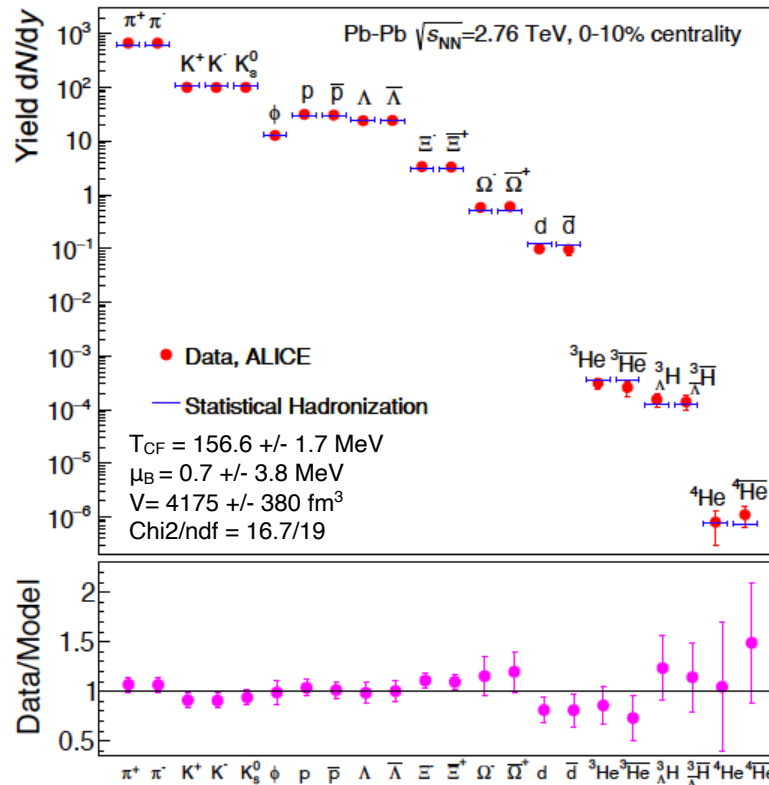


STAR : Phys. Rev. C 96, 044904 (2017).
 STAR : Phys. Rev. C 102, 034909 (2020).

THERMUS: S. Wheaton, J. Cleymans Comp.
 Phys. Comm. 180, 84 (2009)

$$\ln Z^{GC}(T, V, \{\mu_i\}) = \sum_{\text{species } i} \frac{g_i V}{(2\pi)^3} \int d^3p \ln(1 \pm e^{-\beta(E_i - \mu_i)})^{\pm 1}$$

$$N_i^{GC} = T \frac{\partial \ln Z^{GC}}{\partial \mu_i} = \frac{g_i V}{2\pi^2} \sum_{k=1}^{\infty} (\mp 1)^{k+1} \frac{m_i^2 T}{k} K_2\left(\frac{km_i}{T}\right) \times e^{\beta k \mu_i}$$

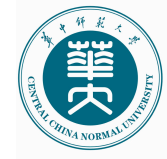


Andronic, Braun-Munzinger, Redlich, Stachel, Nature 561, 321 (2018).

Features of thermal model:

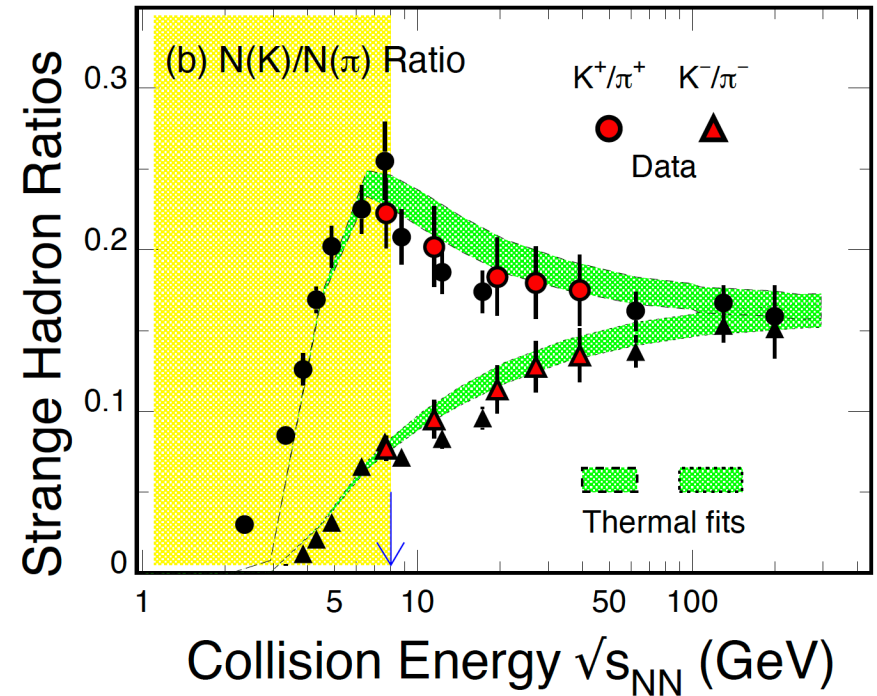
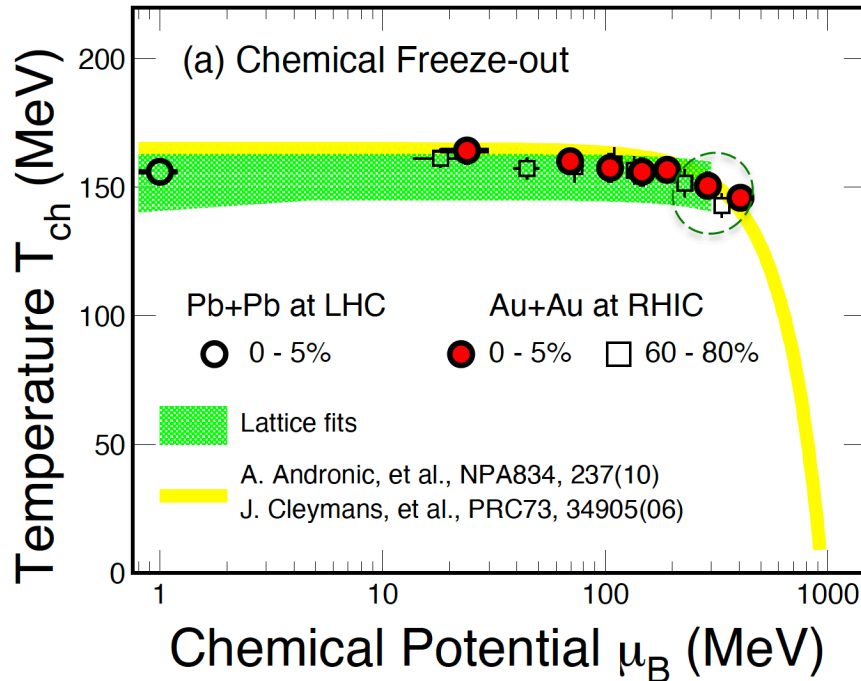
- Non-interacting hadrons and resonances
- Thermodynamically equilibrium system

Dynamics characterized by:
 Temperature T_{ch} and
 baryon chemical potential μ_B



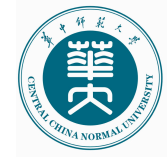
Chemical freeze-out and QCD phase boundary

By courtesy of Dr. N. Xu

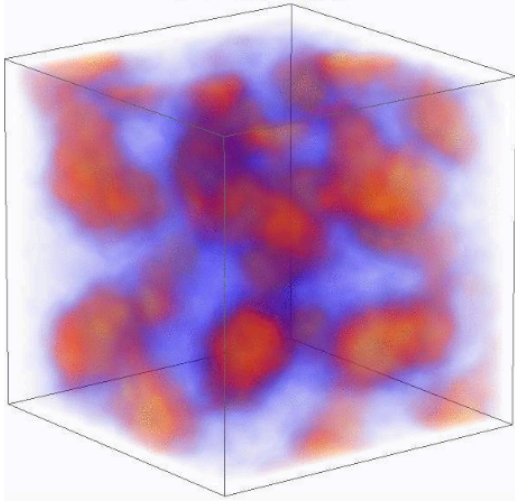


- The chemical freeze-out T and μ_B (GCE) are close to the phase boundary determined from Lattice QCD with $\mu_B < 300$ MeV.
- The peak of K^+/π^+ ratio around 8 GeV can be well described by thermal model, where the system start to enter into “high baryon density region”. (< 8 GeV, $\mu_B > 420$ MeV)

STAR : PRC96, 044904 (2017); PRC 102, 034909 (2020). ALICE : PRL 109, 252301 (2012), PRC 88, 044910 (2013).
A. Andronic, P. Braun-Munzinger, K. Redlich, J. Stachel, Nature 561, 321 (2018). X. Luo, S. Shi, N. Xu and Y. Zhang, Particle 3, 278 (2020); K. Fukushima, B. Mohanty, N. Xu, arXiv: 2009.03006; J. Randrup et al., Phys. Rev. C74, 047901(2006).



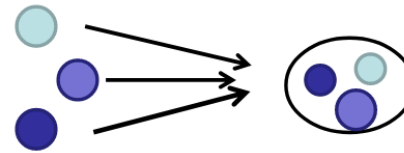
Sensitive observables for QCD phase transition



In the vicinity of critical point and/or 1st order phase transition



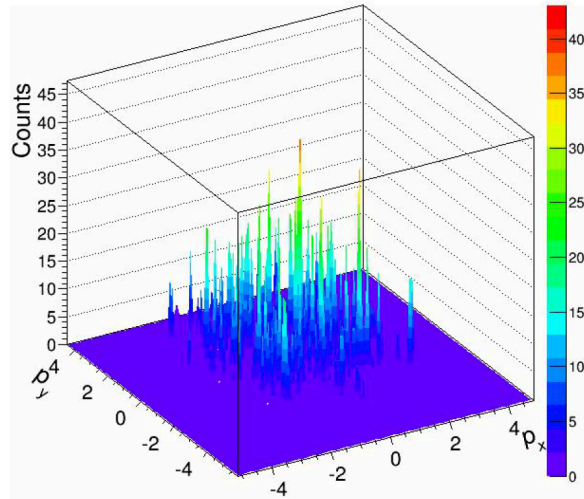
Large density fluctuations and Baryon clustering



Higher moments of conserved charge (B, Q, S) distributions

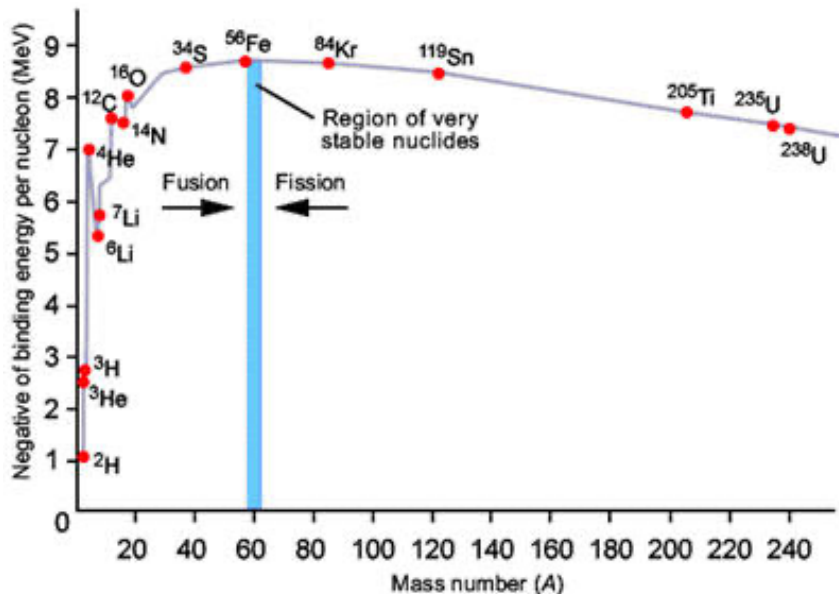
light nuclei and hypernuclei production

Experimental Signatures:
Non-monotonic variation as a function of collision energy.

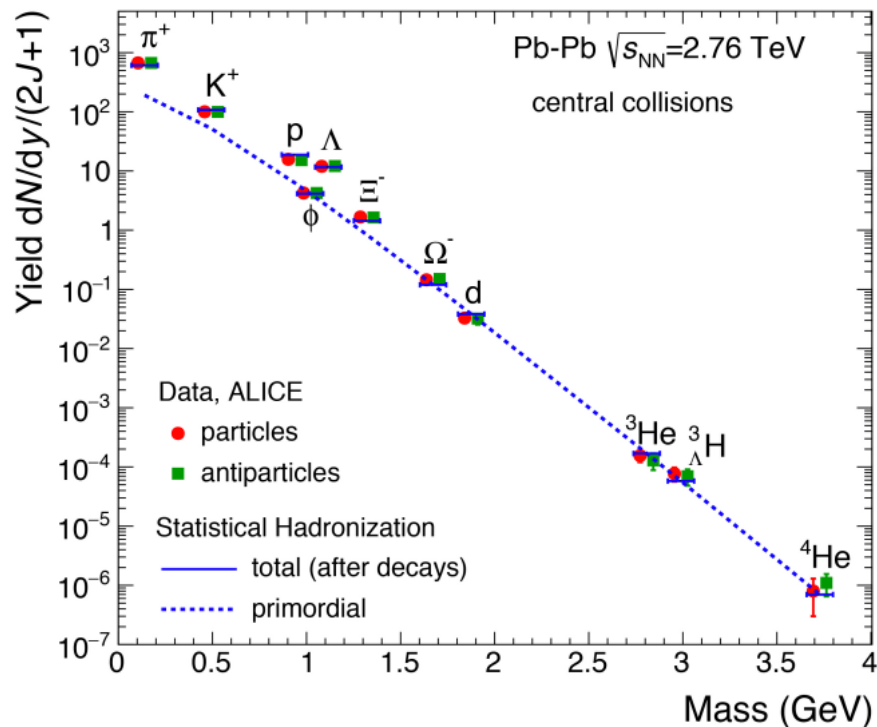




Light Nuclei production in high energy nuclear collisions



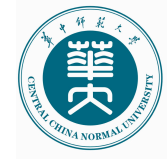
nucleus	rms radius (fm)
deuteron	2.1421 ± 0.0088
triton	1.7591 ± 0.0363
^3He	1.9661 ± 0.0030
^4He	1.6755 ± 0.0028
^3H	4.9
Λ	



“Snowball in hell” ?

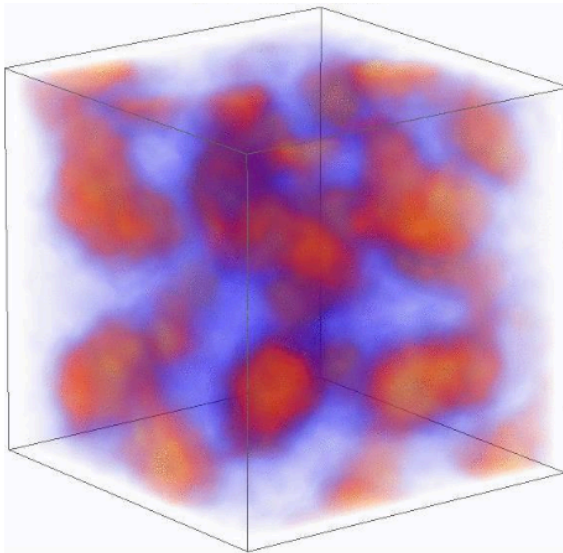
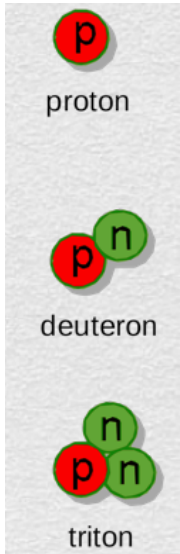
- Light nuclei (d, t, ^3He): loosely bond object with few MeV binding energies can be produced in HIC.
- Understanding the production mechanism of light nuclei in HIC will provide baseline to map the QCD phase boundary. coalescence、microscopic interactions、 thermal production ?

Braun-Munzinger, Dönigus, NPA 987, 144 (2019).
 Benjamin Dönigus, IJMPE 29, 2040001 (2020).
 J. Chen, et al., Phys. Rep. 760, 1 (2018)
 D. Oliinychenko, et al., Phys. Rev. C 99, 044907 (2019).
 Y. Oh, Z.W. Lin, C.M. Ko, Phys. Rev. C 80, 064902 (2009).
 S. Sombun et al., Phys. Rev. C 99,014901 (2019).



Light nuclei production as probes of QCD phase structure

Near first order P.T. or critical point :
large density fluctuations and baryon clustering



Based on coalescence model:

$$N_d = \frac{3}{2^{1/2}} \left(\frac{2\pi}{m_0 T_{eff}} \right)^{3/2} N_p \langle n \rangle (1 + C_{np})$$

$$N_t = \frac{3^{3/2}}{4} \left(\frac{2\pi}{m_0 T_{eff}} \right)^3 N_p \langle n \rangle^2 (1 + \Delta n + 2C_{np})$$

New observable : Yield ratio of light nuclei

$$N_t \cdot N_p / N_d^2 \approx g(1 + \Delta n)$$

Neutron density fluctuations $\Delta n = \langle (\delta n)^2 \rangle / \langle n \rangle^2$
 $g=0.29$

Yield ratio of light nuclei is sensitive to the baryon density fluctuations and can be used to probe the signature of 1st order phase transition and/or critical point in heavy-ion collisions.

K.J. Sun, L.W. Chen, C.M. Ko, and Z.B. Xu, PLB 774, 103 (2017);

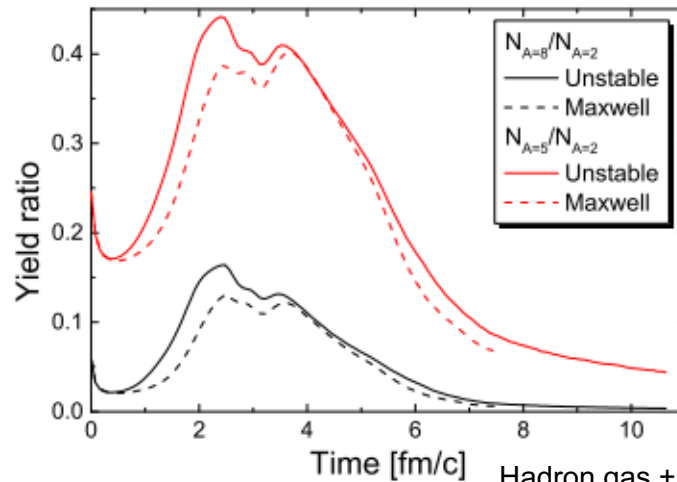
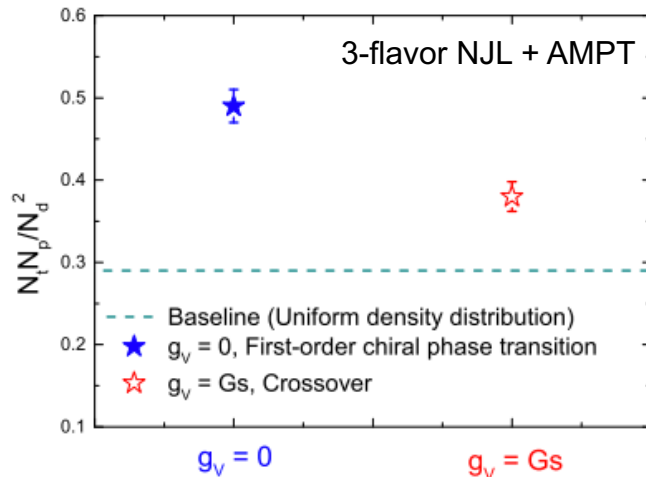
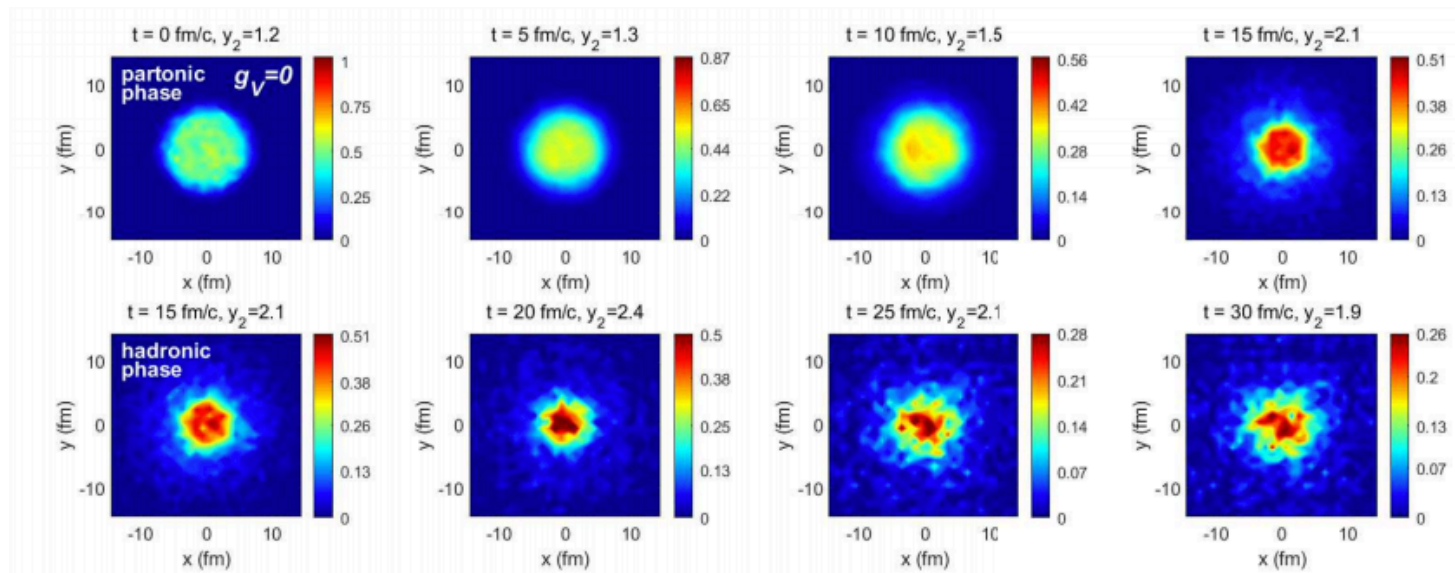
K.J. Sun, L.W. Chen, C.M. Ko, J. Pu, and Z.B. Xu, PLB781, 499 (2018)

Edward Shuryak, Juan M. Torres-Rincon, PRC 100, 024903 (2019); PRC 101, 034914 (2020); EPJA 56, 241 (2020).



Effects of 1st order phase transition : Yield ratio of light nuclei

First order phase transition : evolution of net-baryon number density at $z=0$

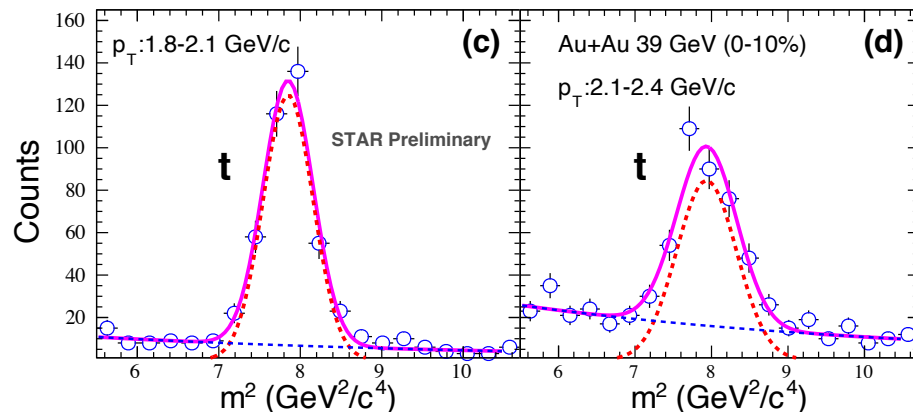
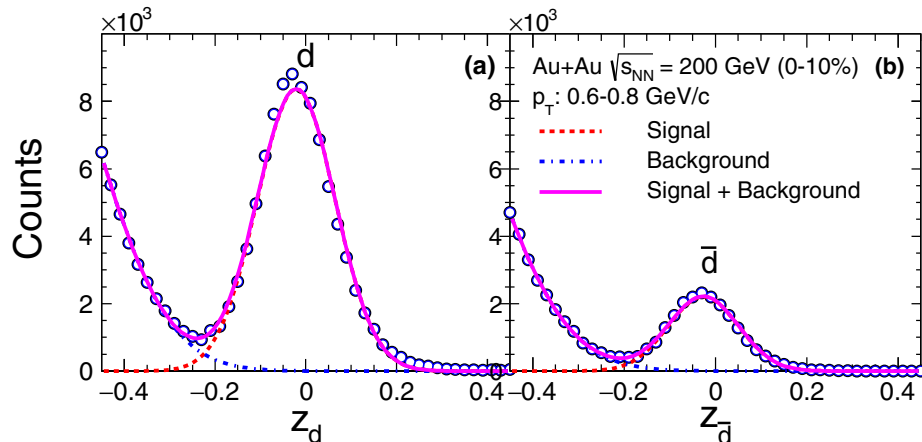
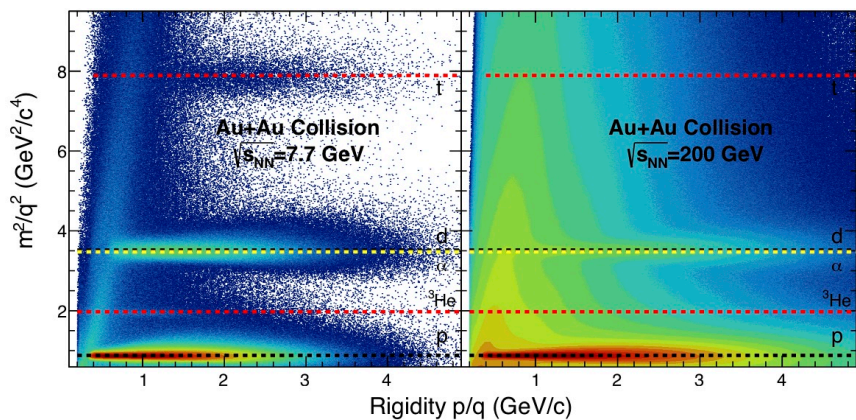
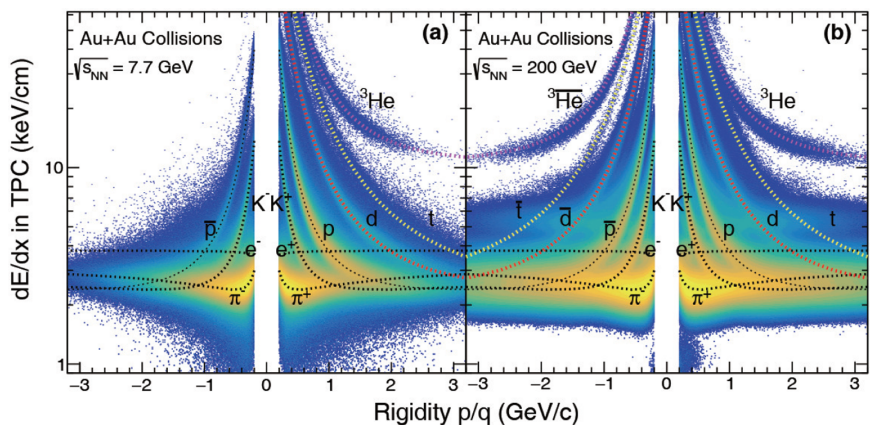


K. J. Sun, C. M. Ko, F. Li, J. Xu, L. W. Chen, arXiv: 2006.08929 J. Steinheimer, J. Randrup, V. Koch, Phys. Rev. C 89, 034901 (2014)



Particle Identification

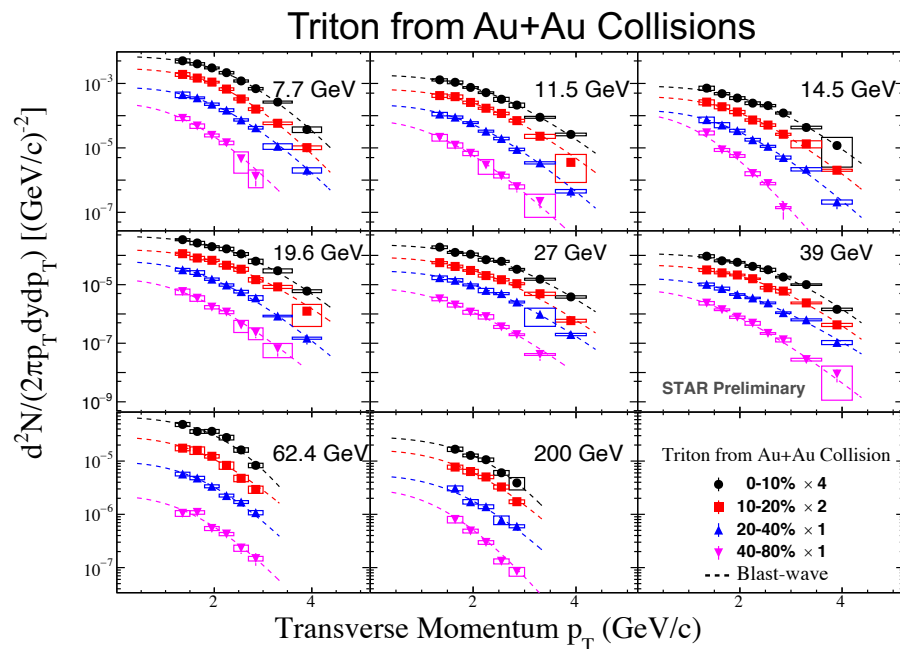
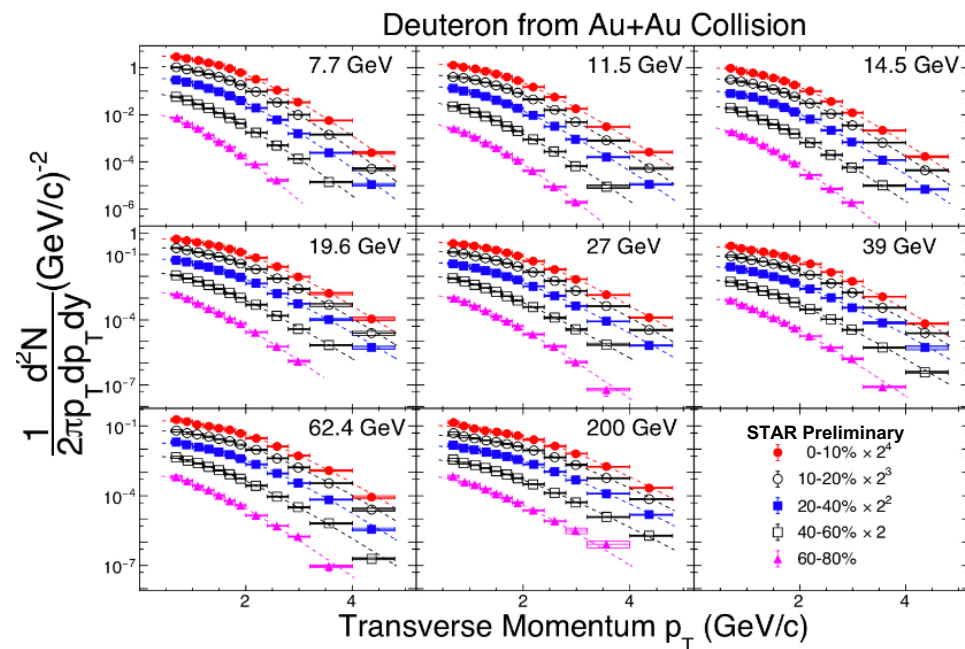
TPC : Low p_T TPC+TOF : High p_T



- 1) TPC and TOF efficiency correction
- 2) Energy loss corrections
- 3) Absorption corrections
- 4) Background subtraction



Deuteron and triton production from BES-I at RHIC



Dash lines (blast-wave function fits) : $\frac{d^2N}{p_T dp_T dy} \propto \int_0^R r dr m_T I_0 \left(\frac{p_T \sinh \rho}{T} \right) K_1 \left(\frac{m_T \cosh \rho}{T} \right)$

E. Schnedermann, J. Sollfrank, and U. Heinz, PRC 48,2462 (1993).

STAR BES-I data :

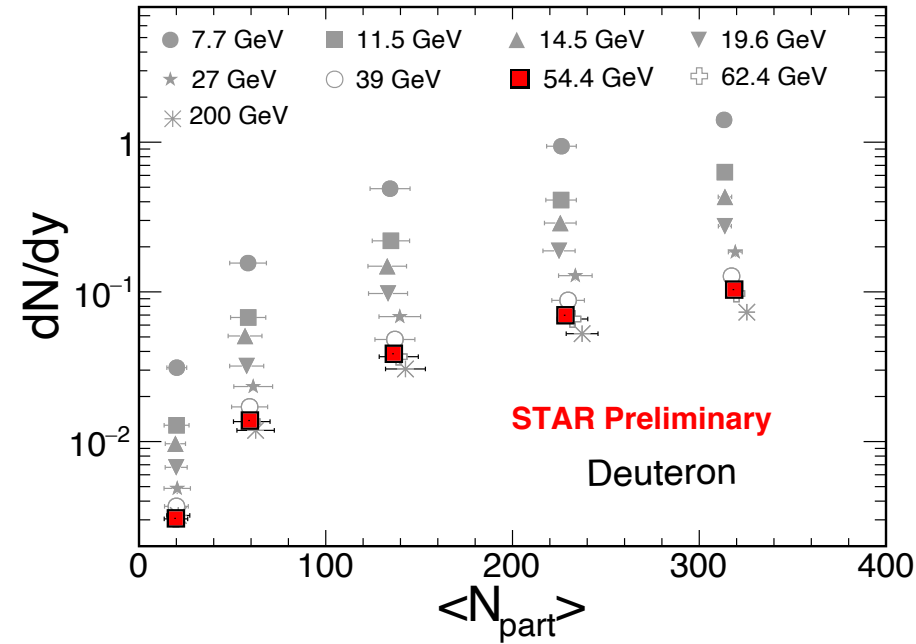
Deuteron, Phys. Rev. C 99, 064905 (2019).

Triton : Dingwei Zhang (for STAR), QM2019 [arXiv : 2002.10677]; Hui Liu, Poster, QM2019.

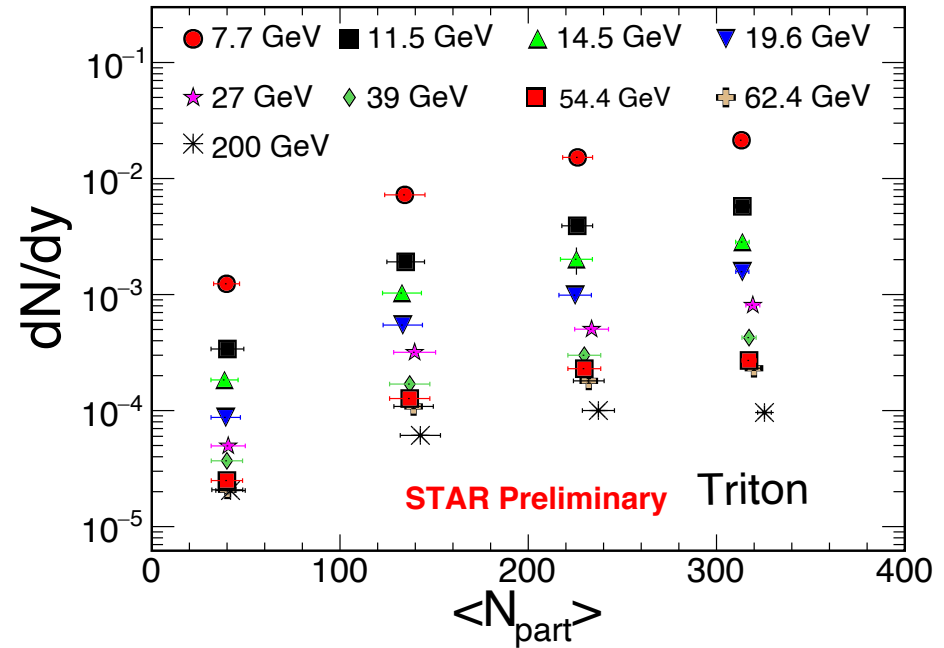


Deuteron and Triton dN/dy from RHIC BES-I

Deuteron



Triton



- Increases with decreasing energy: baryon stopping.
- Increases from peripheral to central collisions.

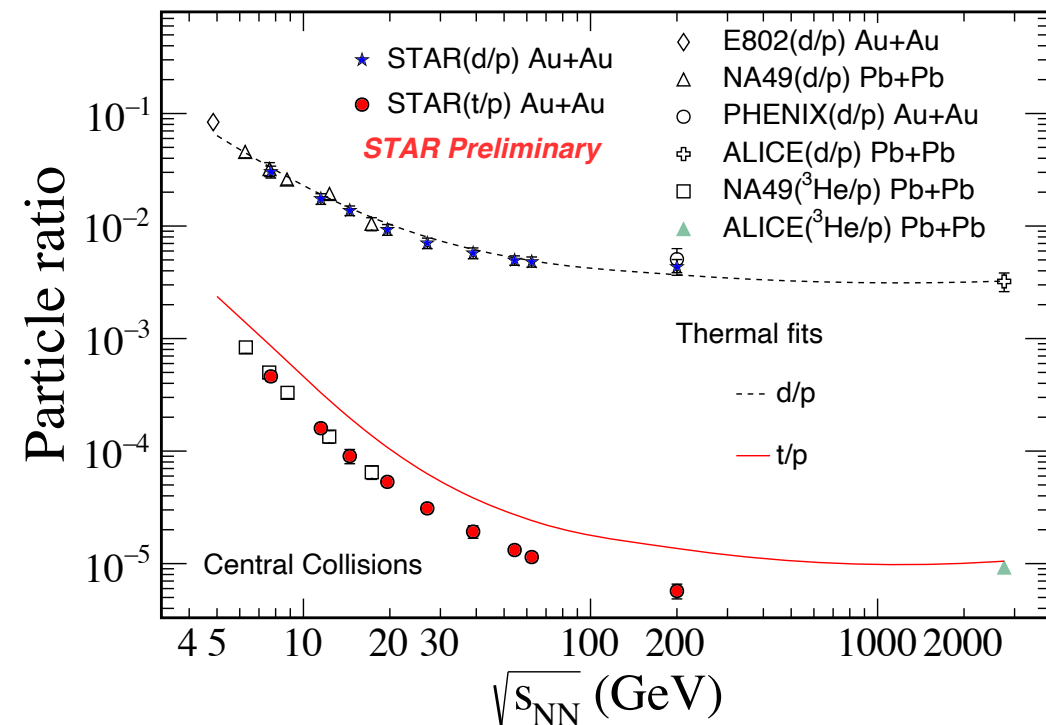
STAR BES-I data :

Deuteron, Phys. Rev. C 99, 064905 (2019).

Triton : Dingwei Zhang (for STAR), QM2019 [arXiv : 2002.10677]; Hui Liu, Poster, QM2019.



Energy dependence of d/p and t/p ratios



Thermal model inputs:

$$T_{CF} = T_{CF}^{lim} / (1 + \exp(2.60 - \ln(\sqrt{s_{NN}})/0.45))$$

$$\mu_B = a / (1 + 0.288\sqrt{s_{NN}})$$

With $\sqrt{s_{NN}}$ in GeV

$$T_{CF}^{lim} = 158.4 \text{ MeV and } a = 1307.5 \text{ MeV}$$

A. Andronic, P. Braun-Munzinger, J. Stachel,
H. Stöcker, PLB 697 (2011) 203.

Proton yield corrected for weak decay feed down
based on a STAR paper using UrQMD + GEANT simulation :
<https://journals.aps.org/prl/supplemental/10.1103/PhysRevLett.121.032301>

- The d/p ratios from LHC、RHIC down to AGS energies can be well described by thermal model.
- t/p and $^3\text{He}/p$ ratios are significant deviation and below the thermal model expectations at RHIC and SPS energies.

ALICE data : Phys. Rev. C 93, 024917 (2016)

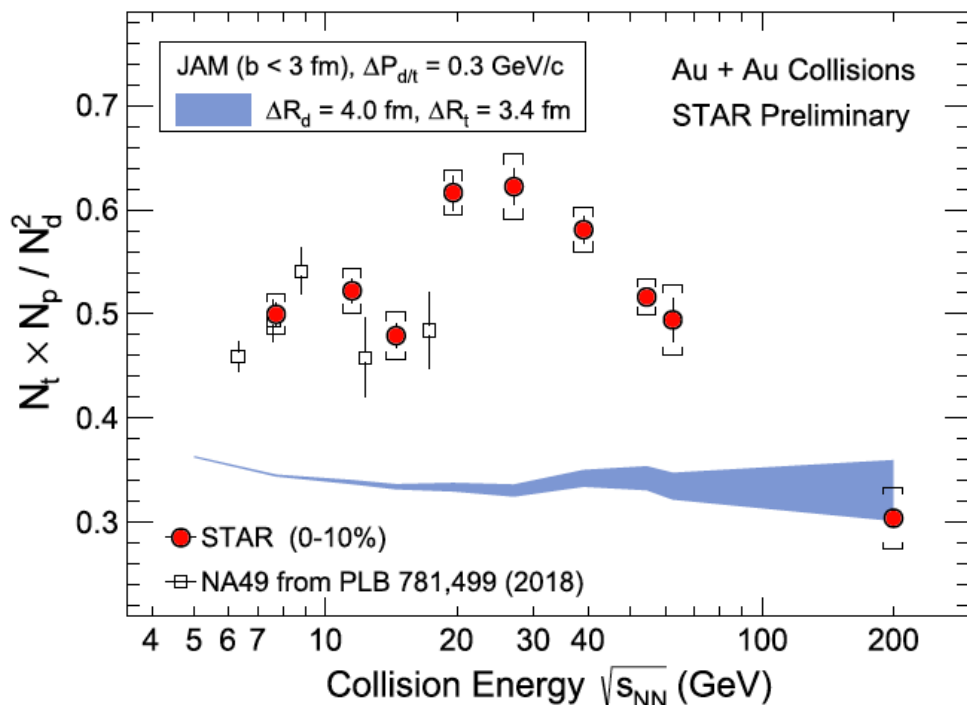
STAR data : Deuteron, Phys. Rev. C 99, 064905 (2019).

Triton : Dingwei Zhang (for STAR), QM2019 [arXiv : 2002.10677]; Hui Liu, Poster, QM2019.



Energy Dependence of Light Nuclei Yield Ratio

Dingwei Zhang (STAR), QM2019 [arXiv: 2002.10677]



The yield ratio is related to neutron density fluctuations.

$$N_t \cdot N_p / N_d^2 = g(1 + \Delta n),$$

with $g = 0.29$

Proton yield corrected for weak decay feed down used in the left plot based on a STAR paper using UrQMD + GEANT simulation : <https://journals.aps.org/prl/supplemental/10.1103/PhysRevLett.121.032301>

A hybrid model treatment of proton weak decay correction and microscopic production of deuteron via pion catalysis : D. Oliinychenko, C. Shen and V. Koch, arXiv: 2009.01915

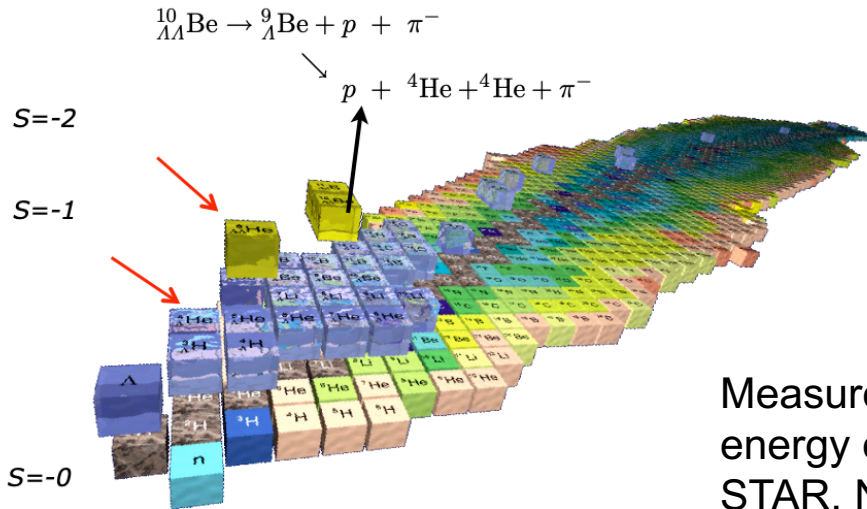
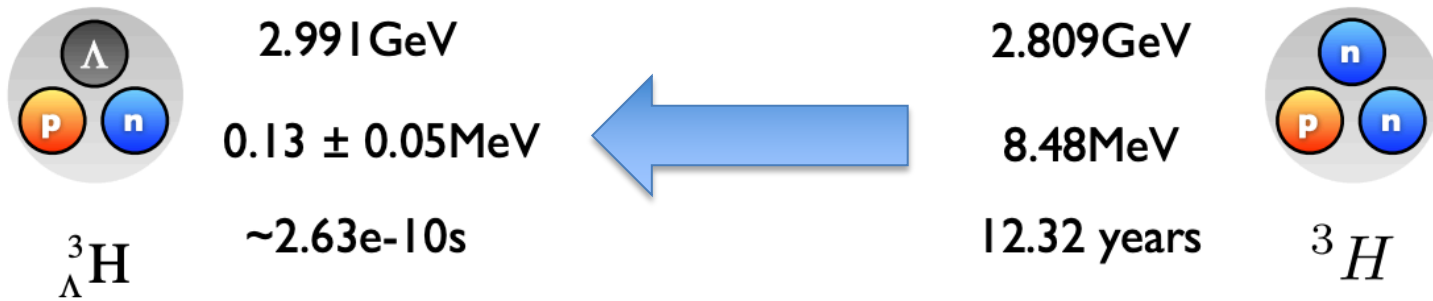
- Yield ratio shows a non-monotonic dependence on collision energy in 0-10% Au + Au collisions, with a peak around 20-30 GeV.
- Flat energy dependence of yield ratio observed in JAM, AMPT, UrQMD, hybrid model.

JAM : H. Liu et al, Phys. Lett. B 805, 135452 (2020).
AMPT : K. Sun, C. M. Ko, arXiv: 2005.00182.

Hydro + transport + coal. : W. Zhao et al., arXiv: 2009.06959
UrQMD: X. G. Deng, Y. G. Ma, Phys. Lett. B 808, 135668 (2020)



Hypernucleus : A New Dimension to the World of Nuclei



Observation of an Antimatter Hypernucleus
STAR, Science 328, 58 (2010)

Measurement of the mass difference and the binding energy of the hypertriton and antihypertriton
STAR, Nature Physics 16, 409 (2020)

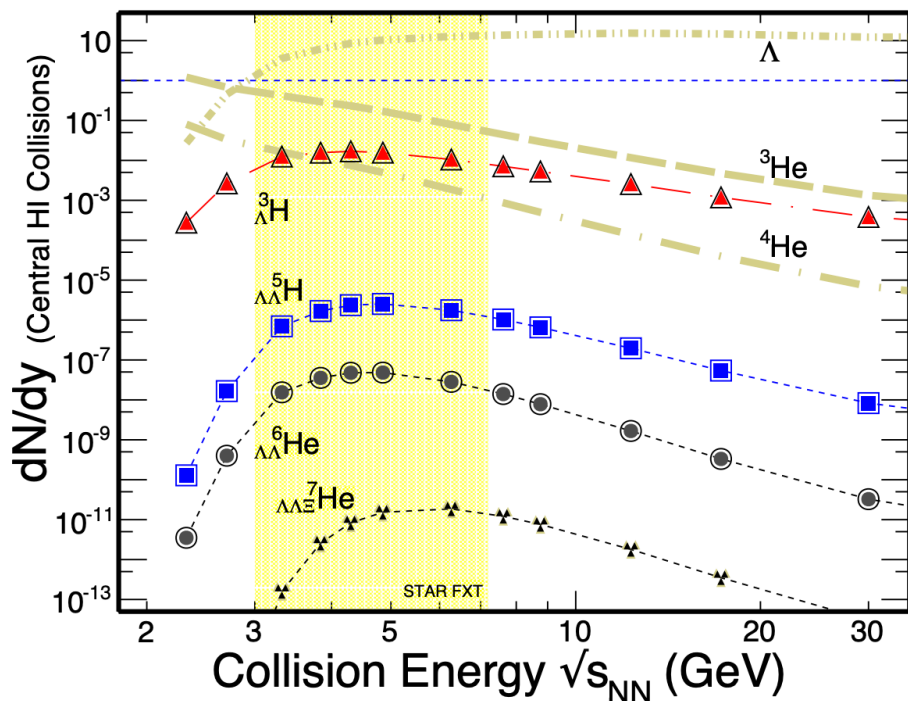
Hypernucleus provides an indirect way to study Y-N interaction

Important to understand strong interaction and EoS of neutron stars

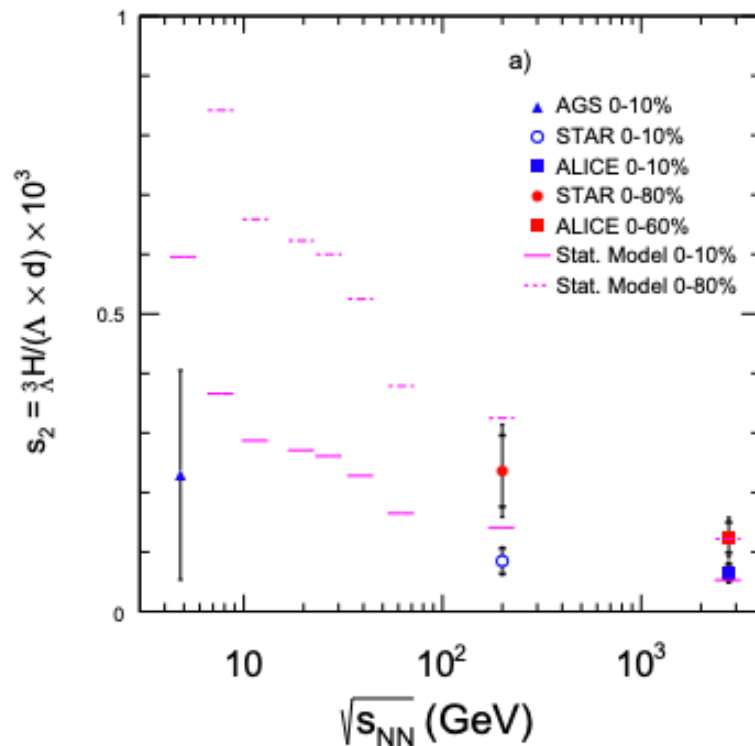


Production of hypernucleus and yield ratios

Thermal model



A. Andronic et al., Phys. Lett. B 697, 203 (2011)
 J. Steinheimer et al., Phys. Lett. B 714, 85 (2014)
 K. Fukushima, B. Mohanty, N. Xu, arXiv: 2009.03006



T. Shao et al., arXiv : 2004.02385 (Accepted by CPC)

Strangeness population factor :

$$S_3 = \frac{^3\Lambda\text{H}}{^3\text{He} \times \Lambda/p}$$

PRL 95(2005) 182301, PRC 74(2006) 054901,
 PRD 73(2006)014004; S.Zhang et al., PLB 684 (2010) 224

Recently Proposed: $S_2 = \frac{N_{^3\Lambda\text{H}}}{N_{\Lambda}N_d}$

Sensitive to local baryon-strangeness correlation.



Fluctuations Probes the QCD Phase Transition

1. Fluctuations signals the QCD Critical Point.

M. Stephanov, K. Rajagopal, E. Shuryak, Phys. Rev. Lett. 81, 4816 (1998).

M. Stephanov, K. Rajagopal, E. Shuryak, Phys. Rev. D 60, 114028 (1999).

Probe singularity of the equation of state: Divergence of the fluctuations.

2. Fluctuations signals the Quark Deconfinement.

S. Jeon and V. Koch, Phys. Rev. Lett. 85, 2076(2000).

M. Asakawa, U. Heinz and B. Muller, Phys. Rev. Lett. 85, 2072 (2000).

Proposed experimental observables:

1. Pion multiplicity fluctuations.
2. Mean p_T fluctuations.
3. Particle ratio fluctuations



Fluctuations and Correlations

Two-point correlation functions of magnetic moment:

$$G(\vec{r}) = \langle S(\vec{r})S(0) \rangle - \langle S(\vec{r}) \rangle \langle S(0) \rangle$$

$S(\vec{r})$: Spatial Magnetic moment

In 3D case: $G(\vec{r}) \propto \frac{1}{r} e^{-r/\xi(t)}$ **Correlation length**

$$\xi(t) = \xi_0 |t|^{-1/2}$$

t : reduced temperature

**Susceptibility
(2nd fluctuations)**



Correlation length

$$\chi \propto \int G(\vec{r}) d\vec{r} \propto \xi^2(t)$$



Higher Moments of Conserved Quantities (B, Q, S)

1. Higher order cumulants/moments: describe the shape of distributions and quantify fluctuations. (sensitive to the correlation length (ξ))

$$\langle \delta N \rangle = N - \langle N \rangle$$

$$C_1 = M = \langle N \rangle$$

$$C_2 = \sigma^2 = \langle (\delta N)^2 \rangle$$

$$C_3 = S\sigma^3 = \langle (\delta N)^3 \rangle$$

$$C_4 = \kappa\sigma^4 = \langle (\delta N)^4 \rangle - 3 \langle (\delta N)^2 \rangle^2$$

$$\langle (\delta N)^3 \rangle_c \approx \xi^{4.5}, \quad \langle (\delta N)^4 \rangle_c \approx \xi^7$$

M. A. Stephanov, Phys. Rev. Lett. 102, 032301 (2009).

M. Asakawa, S. Ejiri and M. Kitazawa, Phys. Rev. Lett. 103, 262301 (2009).

M. A. Stephanov, Phys. Rev. Lett. 107, 052301 (2011).

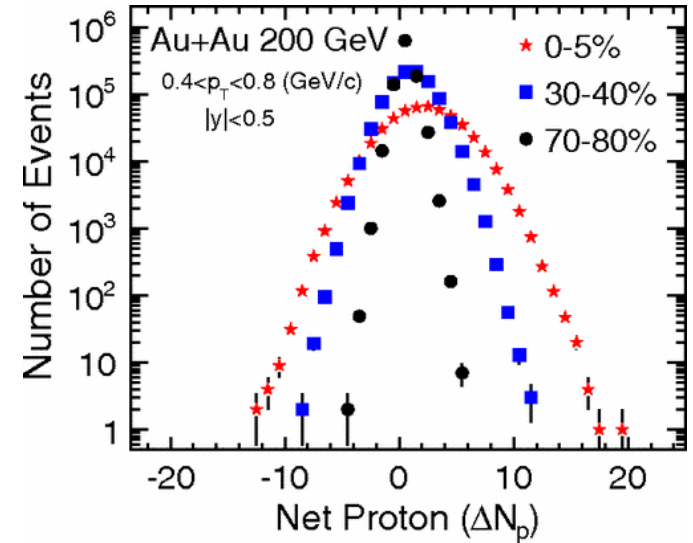
2. Direct connect to the susceptibility of the system.

$$\frac{\chi_q^4}{\chi_q^2} = \kappa\sigma^2 = \frac{C_{4,q}}{C_{2,q}}, \quad \frac{\chi_q^3}{\chi_q^2} = S\sigma = \frac{C_{3,q}}{C_{2,q}},$$

$$\chi_q^{(n)} = \frac{1}{VT^3} \times C_{n,q} = \frac{\partial^n (p/T^4)}{\partial (\mu_q)^n}, \quad q = B, Q, S$$

S. Ejiri et al, Phys. Lett. B 633 (2006) 275. Cheng et al, PRD (2009) 074505. B. Friman et al., EPJC 71 (2011) 1694. F. Karsch and K. Redlich, PLB 695, 136 (2011). S. Gupta, et al., Science, 332, 1525(2012). A. Bazavov et al., PRL109, 192302(12) // S. Borsanyi et al., PRL111, 062005(13)

Event-by-Event Distribution



First Measurement : 2009-2010

STAR, PRL105, 022302 (2010).

➤ **Net-Proton:** $N_p - N_{\bar{p}}$
(proxy: Net-Baryon)

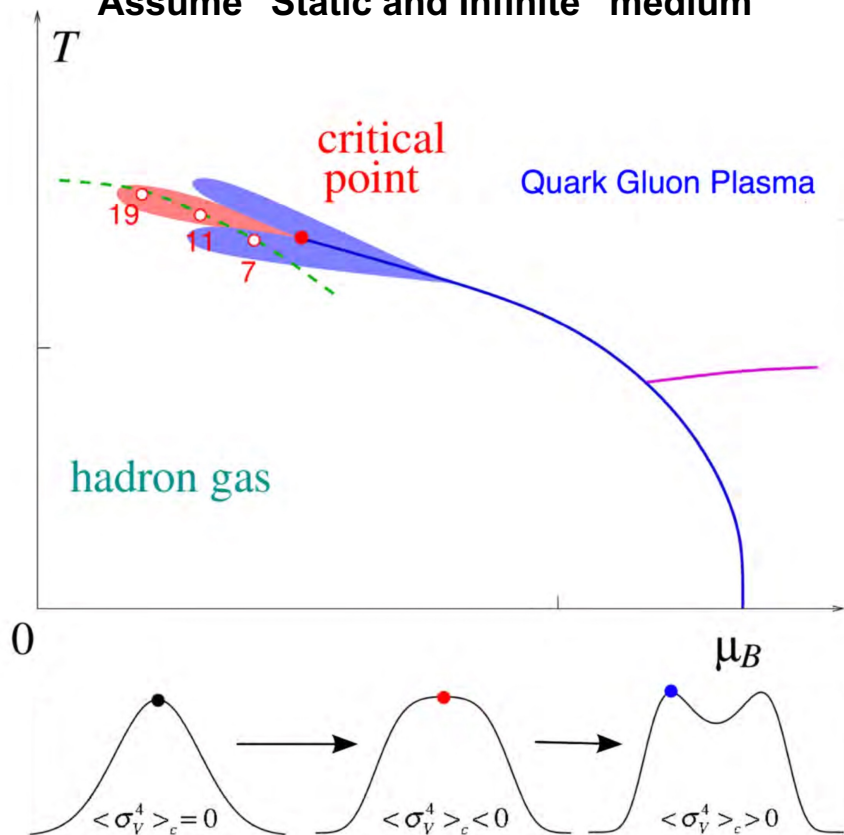
➤ **Net-Charge:** $N_{Q^+} - N_{Q^-}$

➤ **Net-Kaon:** $N_{K^+} - N_{K^-}$
(proxy: Net-Strangeness)



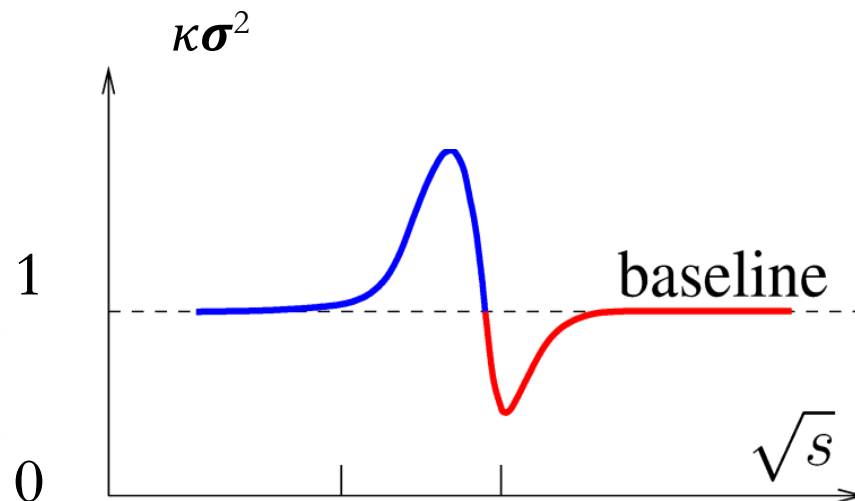
Signals of QCD Critical Point : Theory/Model

Assume "Static and Infinite" medium



Caveats : Non-equilibrium, finite size/time effects

- M. Asakawa, M. Kitazawa, B. Müller, PRC 101, 034913 (2020).
- S Mukherjee, R. Venugopalan, Y Yin, PRL 117, 222301 (2016).
- S. Wu, Z. Wu, H. Song, PRC 99, 064902 (2019).



$$\kappa\sigma^2 = 1 \quad (\text{Poisson Fluctuations})$$

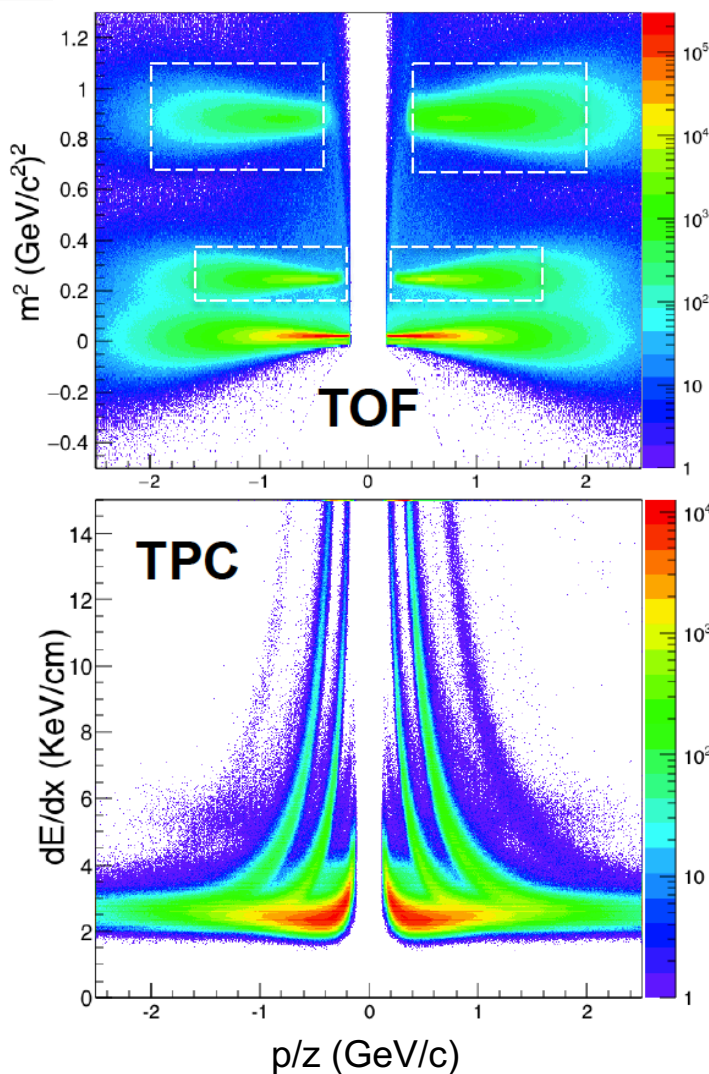
Characteristic signature of CP:
Non-monotonic energy dependence

“Oscillation Pattern”
Especially the Peak at low energies

- M. Stephanov, PRL107, 052301 (2011); J. Phys. G 38, 124147 (2011).
- Schaefer et al., PRD 85, 034027 (2012); W. Fu et al., PRD 94, 116020 (2016).
- J.W. Chen, J. Deng, et al., PRD 93, 034037 (2016). PRD 95,014038 (2017).
- W. K. Fan, X. Luo, H.S. Zong, IJMPA 32, 1750061 (2017);
- G. Shao et al., EPJC 78, 138 (2018) ; Z. Li et al., EPJC 79, 245 (2019).
- A. Bzdak et al., Phys. Rep. 853, 1(2020). D. Mroczek et al, arXiv: 2008.04022.



(Anti-) Proton PID and Acceptance

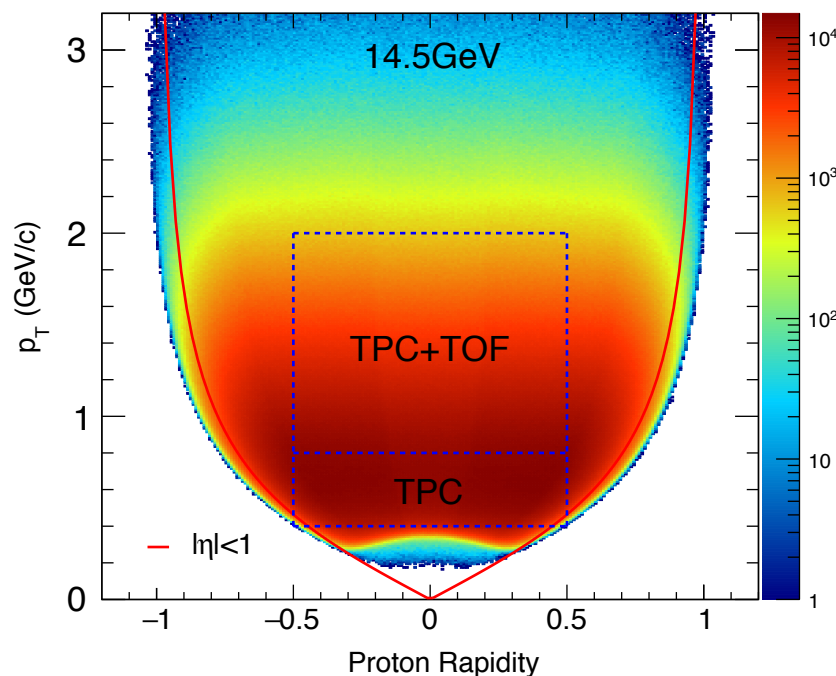


Extend the phase space coverage by TOF.

Doubled the accepted number of proton/anti-proton

$|y| < 0.5$, $0.4 < p_T$ (GeV/c) < 0.8 (Low p_T , TPC PID)

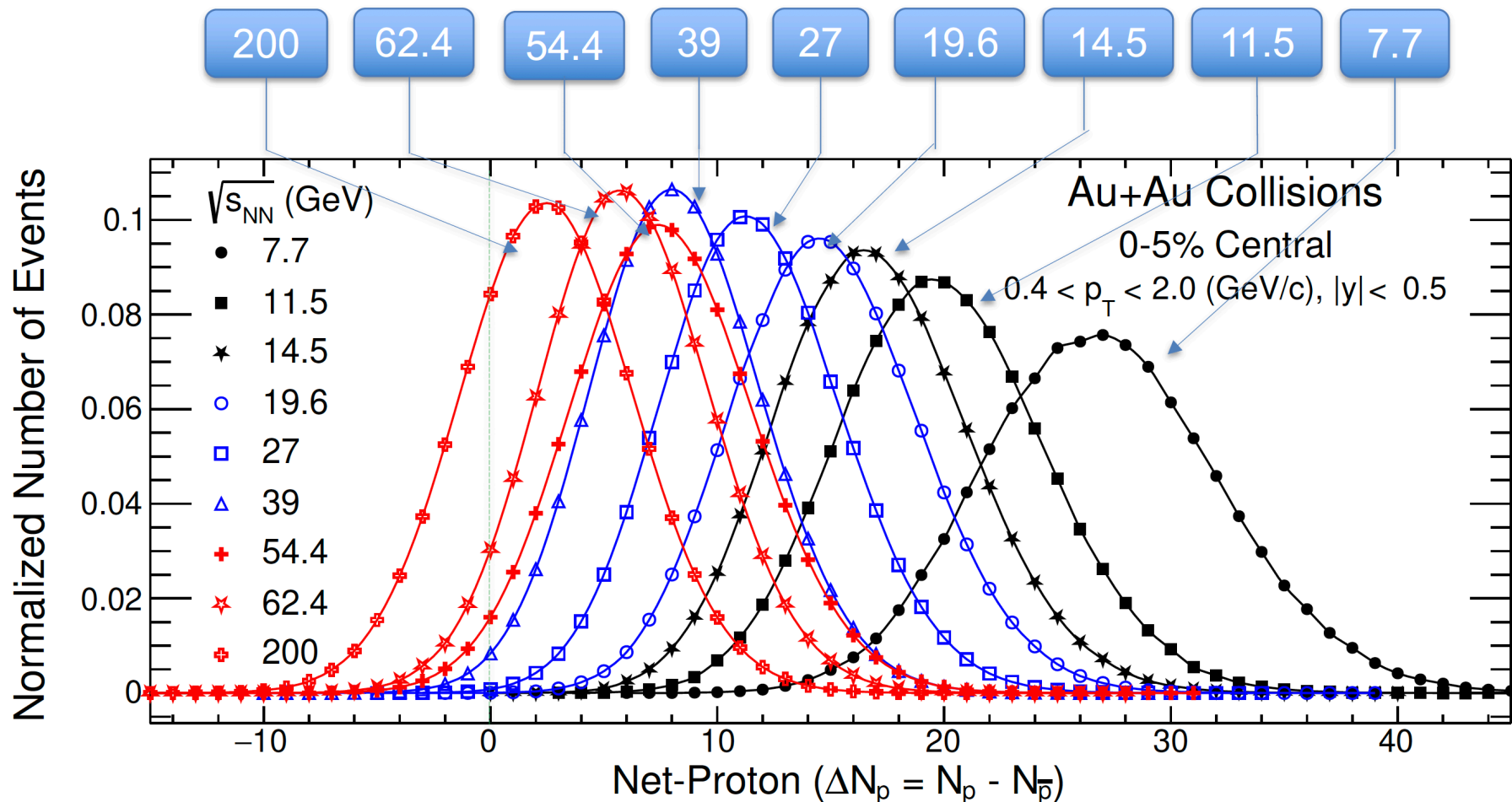
$0.8 < p_T$ (GeV/c) < 2 (High p_T , TPC+TOF PID)



➤ Purity of proton and anti-proton identification $> 97\%$.



Event-by-Event Net-Proton Distributions (0-5%)



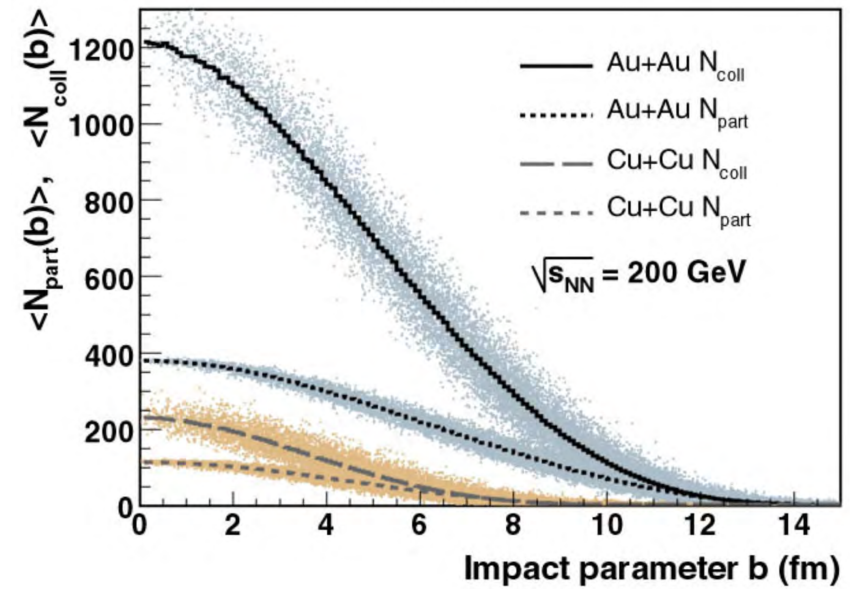
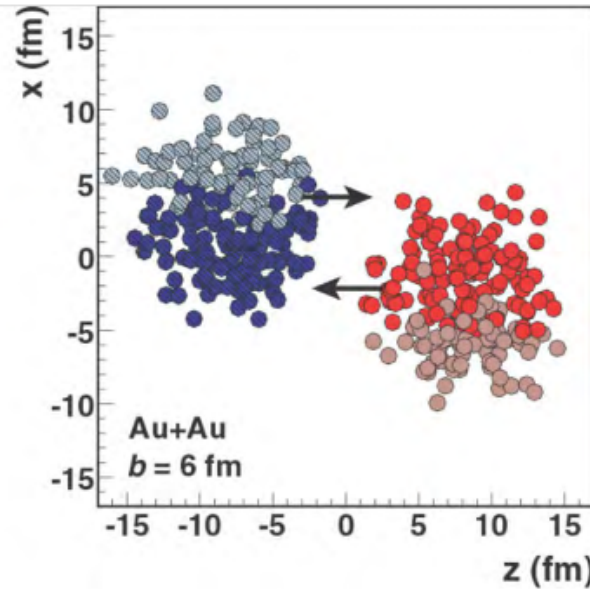
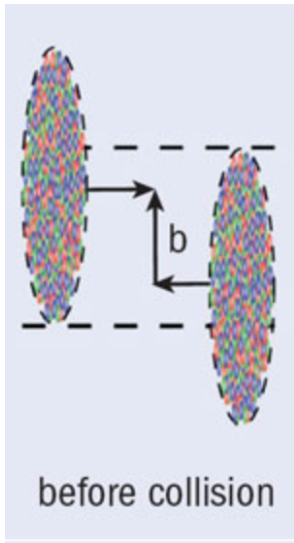
Efficiency uncorrected.

Mean values increase when decreasing energy:

Interplay between baryon stopping and pair production.

STAR, arXiv: 2001.02852

Volume Fluctuations

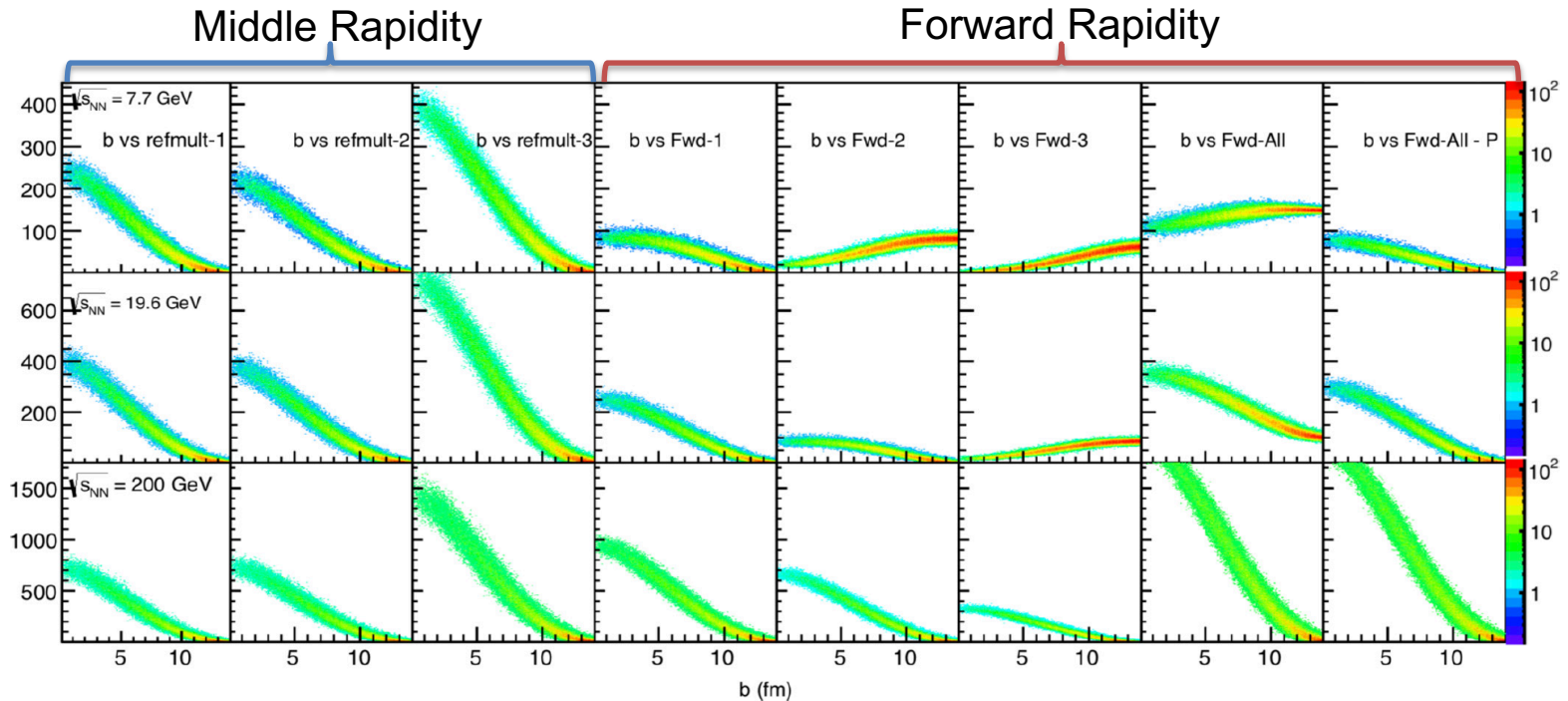


Glauber model: M. L. Miller et al., Ann.Rev.Nucl.Part.Sci.57, 205 (2007)

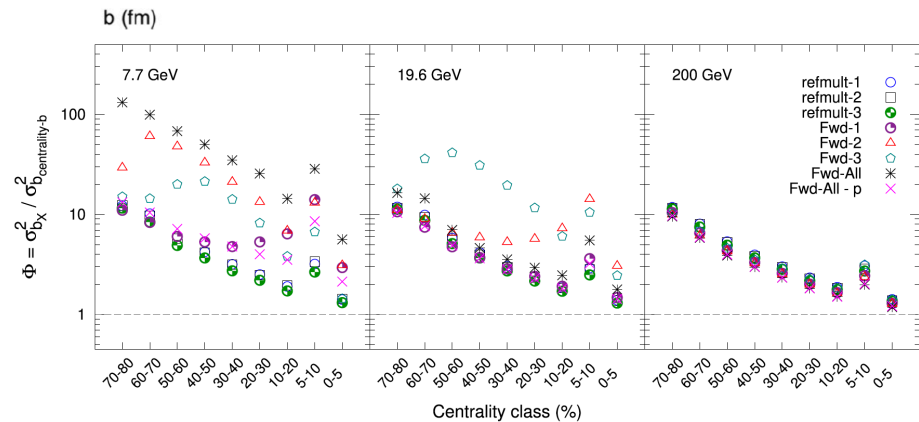
- The quantities (b , N_{part} , N_{coll}) cannot be directly measured.
- Even at fix impact parameters, the number of participant and binary collisions still show large fluctuations.



Centrality Determination and Resolution : UrQMD simulation



Identify	Definition
centrality-b	Impact parameter
refmult-1	N_{ch} within $ \eta < 0.5$
refmult-2	N_{ch} within $0.5 < \eta < 1.0$
refmult-3	$N_{ch} - p$ within $ \eta < 1.0$
Fwd-All	N_{ch} within $2.1 < \eta < 5.1$
Fwd-1	N_{ch} within $2.1 < \eta < 3.0$
Fwd-2	N_{ch} within $3.0 < \eta < 4.0$
Fwd-3	N_{ch} within $4.0 < \eta < 5.0$
Fwd-All - p	$N_{ch} - p$ within $2.1 < \eta < 5.1$

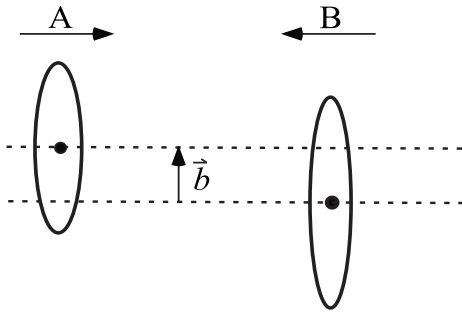


A. Chatterjee, et al., PRC101, 034902 (2020)

- Volume fluctuations are much smaller for most central collisions than mid-central and peripheral collisions.
- At forward region, the mixture of spectator and produced particles will lower the centrality resolution.

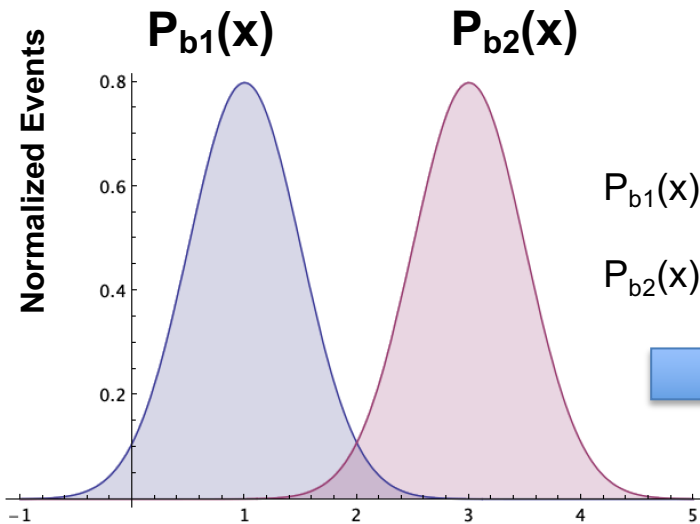


Effects of Volume Fluctuations on Multiplicity Cumulants



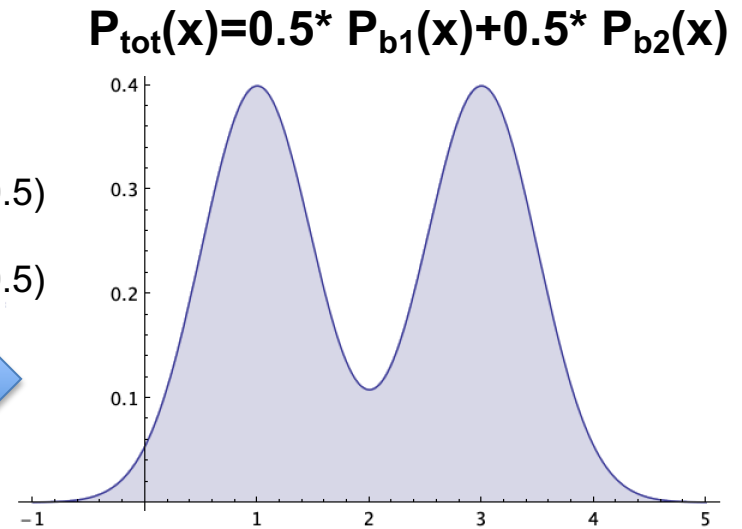
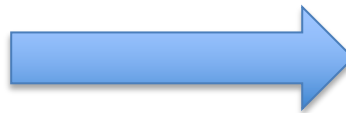
- Even for fixed N_{ch} , impact parameter b still show event-by-event fluctuations.
- Cumulants can be affected by events mixed with different initial impact parameters/participants (volume fluctuations).

P. Zhuang, Lianshou Liu, Phys. Rev. D 42, 848(1990).
Skokov et al., Phys. Rev. C 88, 034911 (2013).
M. Zhou, J. Jia, Phys. Rev. C 98, 044903 (2018).



$$P_{b1}(x) = \text{Gaussian}(1, 0.5)$$

$$P_{b2}(x) = \text{Gaussian}(3, 0.5)$$



$$C_4(P_{b1}) = C_4(P_{b2}) = 0$$

$$C_2(P_{b1}) = C_2(P_{b2}) = 0.25$$

$$C_4/C_2 = 0$$

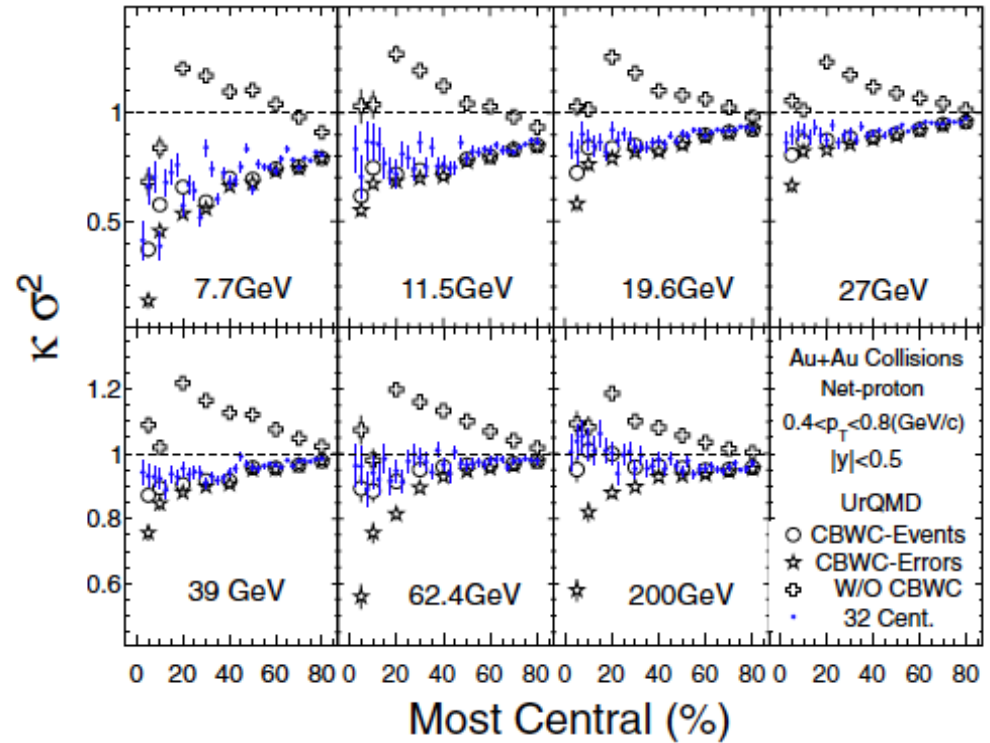
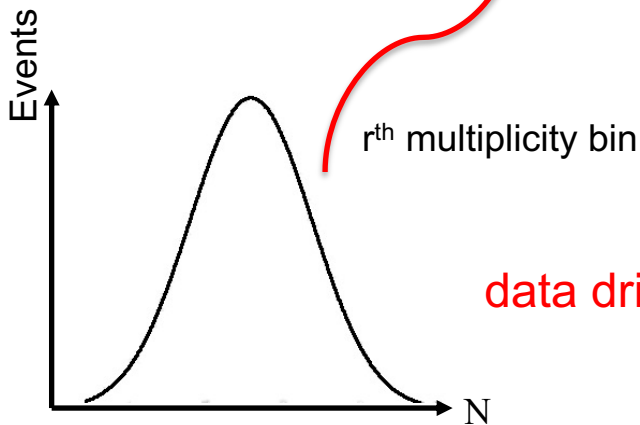
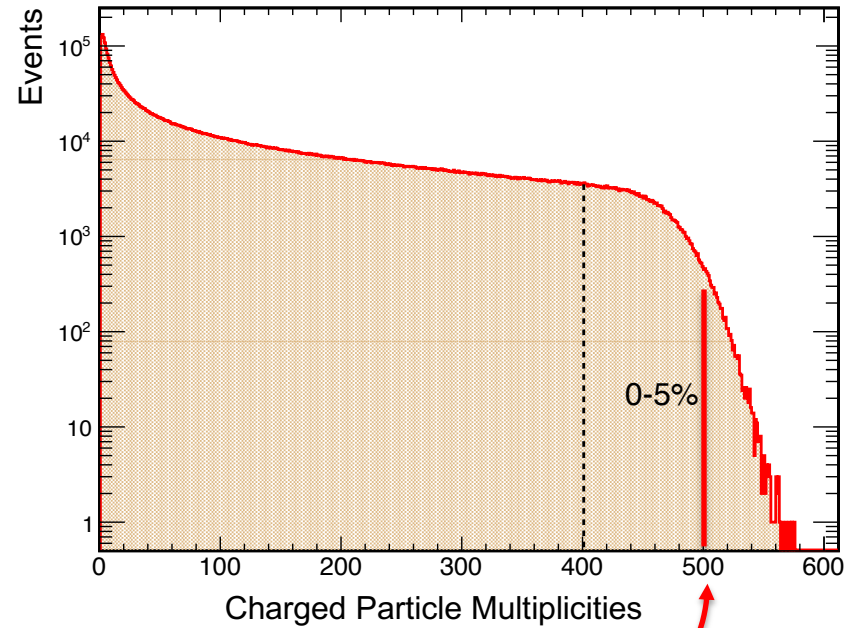
$$C_4(P_{tot}) = -2 \quad C_2(P_{tot}) = 1.25$$

$$C_4/C_2 = -1.6$$



Centrality Bin Width Correction (CBWC)

X.Luo, J. Xu, B. Mohanty and N. Xu. J. Phys. G 40,105104(2013).



$$C_n = \frac{\sum_{r=N_1}^{N_2} n_r C_n^r}{\sum_{r=N_1}^{N_2} n_r} = \sum_{r=N_1}^{N_2} \omega_r C_n^r$$

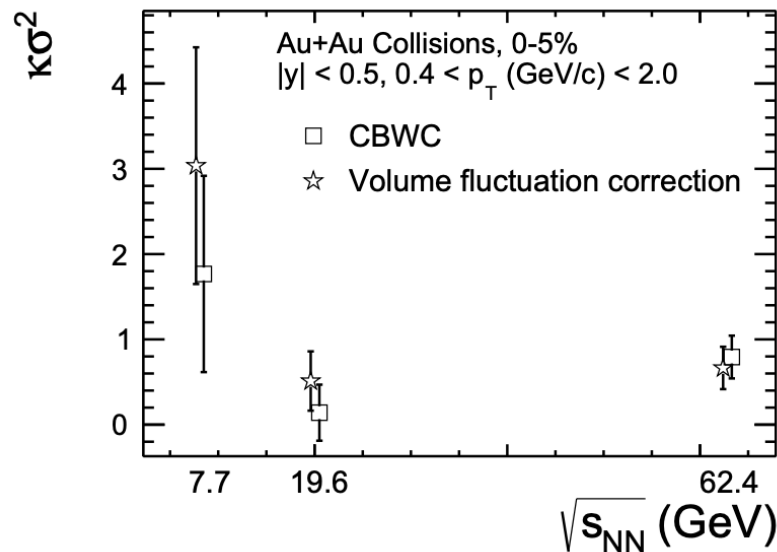
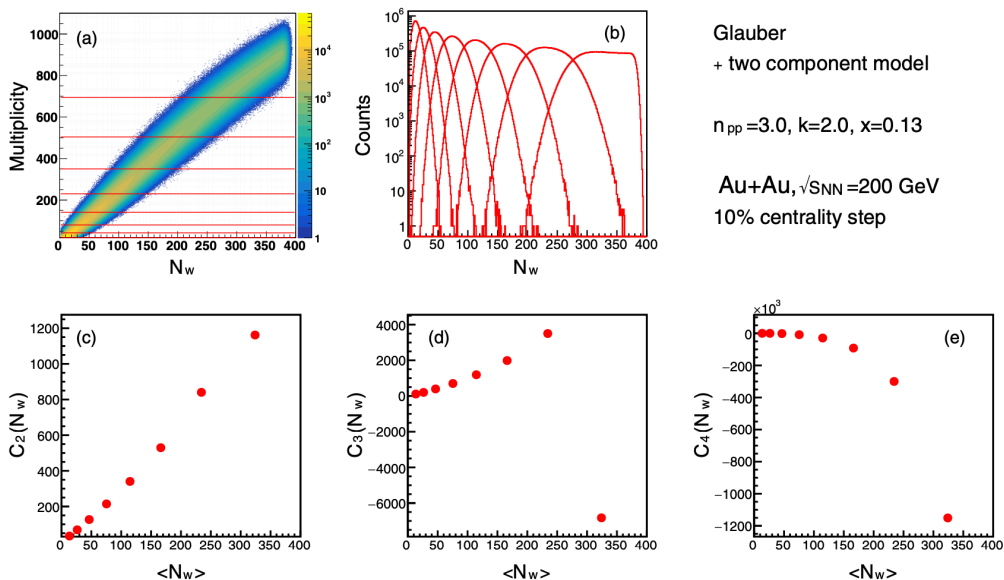
r: rth mul. bin, n_r: number of events in rth bin



Model Dependent Correction Method

➤ Assumption: Independent and Identical emission sources

Glauber model simulation $N = \sum_{N_w} n_i$



$$C_1(N) = \langle N_w \rangle C_1(n)$$

$$C_2(N) = \langle N_w \rangle C_2(n) + \langle n \rangle^2 C_2(N_w)$$

$$C_3(N) = \langle N_w \rangle C_3(n) + 3 \langle n \rangle C_2(n) C_2(N_w) + \langle n \rangle^3 C_3(N_w)$$

$$C_4(N) = \langle N_w \rangle C_4(n) + 4 \langle n \rangle C_3(n) C_2(N_w) + 3 C_2^2(n) C_2(N_w)$$

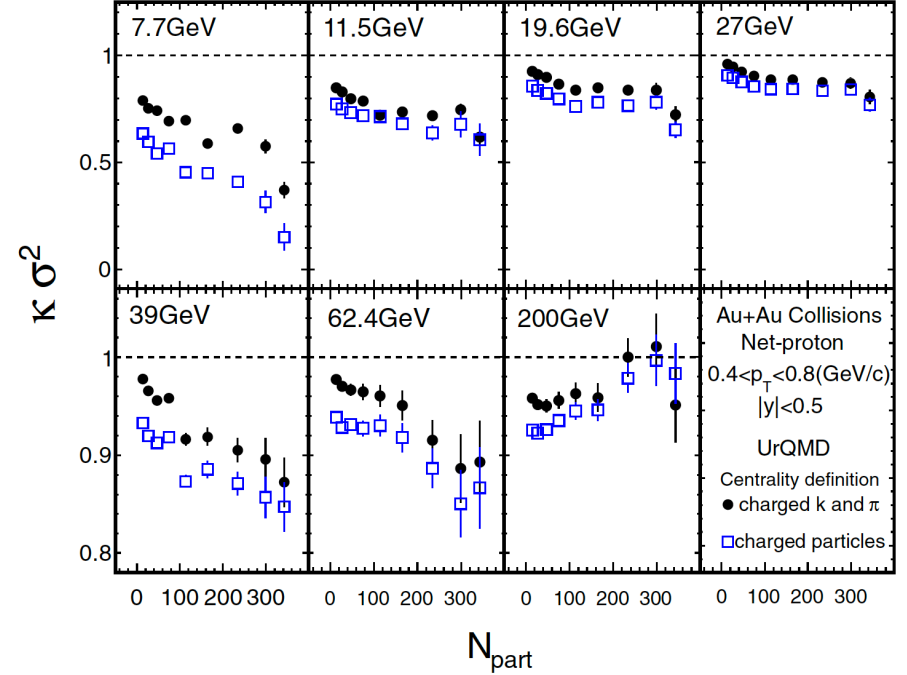
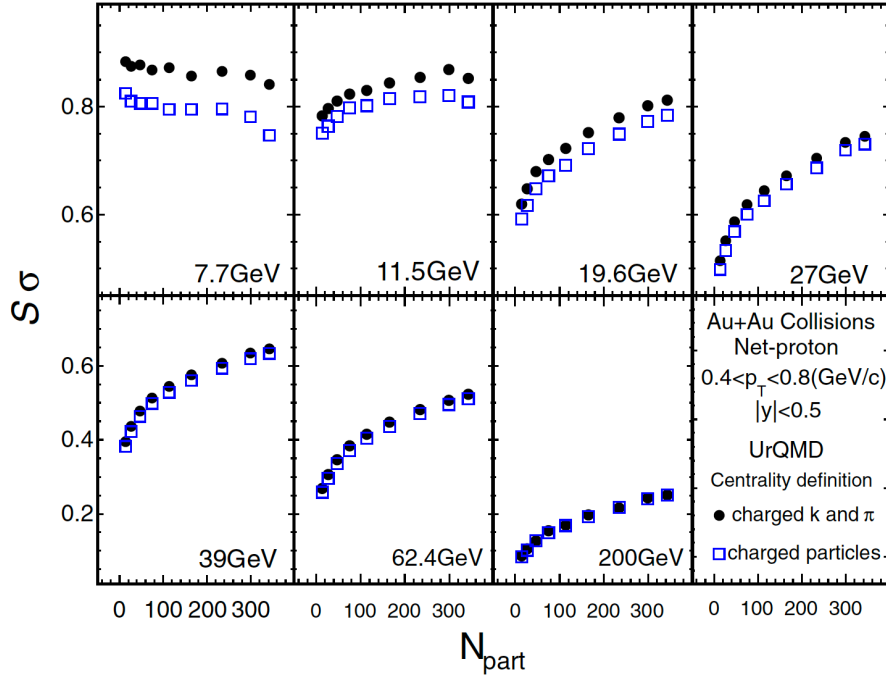
$$+ 6 \langle n \rangle^2 C_2(n) C_3(N_w) + \langle n \rangle^4 C_4(N_w)$$

Results from both CBWC and VFC methods are consistent.

T. Sugiura et al., Phys. Rev. C 100, (2019) 044904
Braun-Munzinger et al., Nucl. Phys. A 960 (2017)114-130
Skokov et al., Phys. Rev. C88 (2013) 034911



Self-correlations



➤ Correlations between particles used in centrality definition and fluctuations.
Methods to suppress/avoid self-correlations:

1) kinematic separation : use particle in different kinematic regions to define centrality.

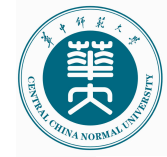
Net-charge fluctuations: [STAR, PRL 113, 092301 \(2014\)](#).

Off-diagonal 2nd order cumulants: [STAR, PRC100, 014902 \(2019\)](#).

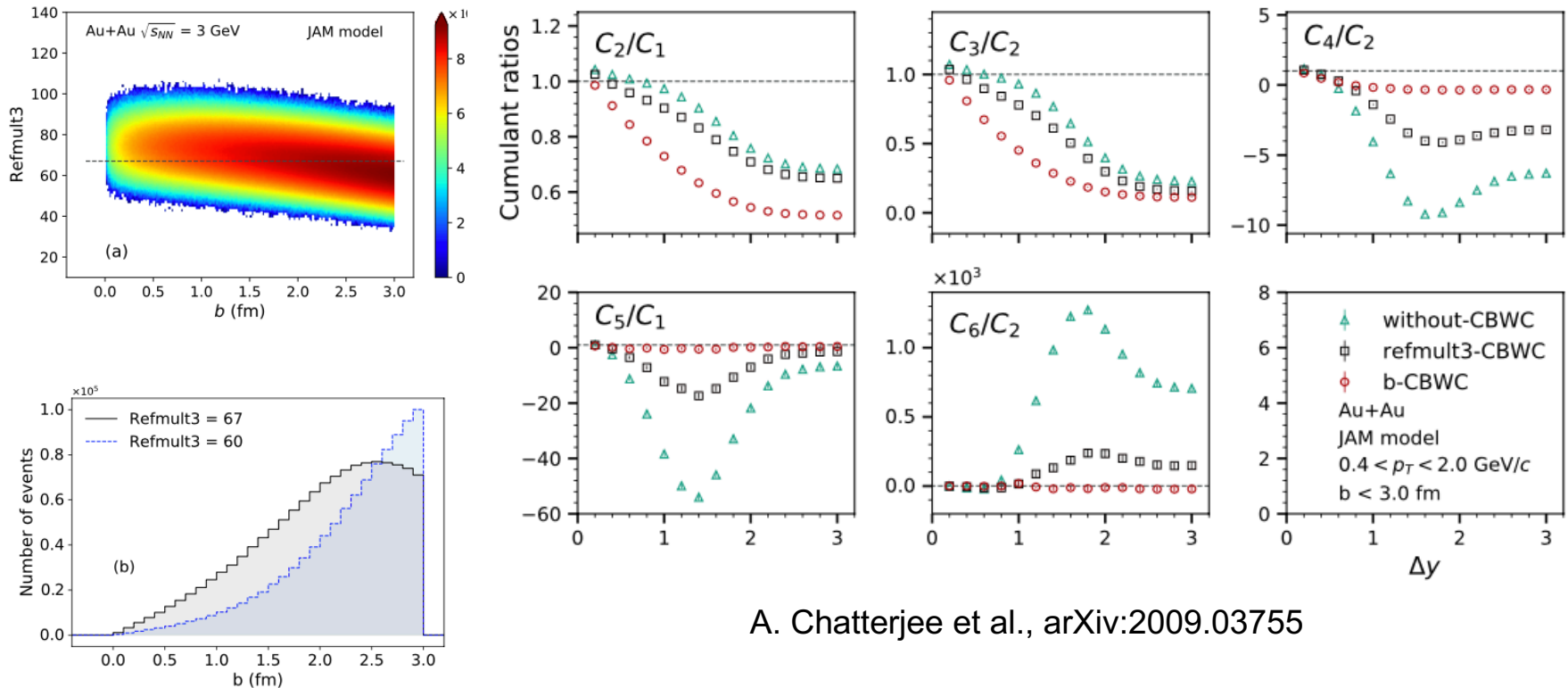
Net-Lambda fluctuations : [STAR, PRC102, 014903 \(2020\)](#).

2) Exclude particles used in fluctuation analysis from the centrality definition

net-proton and net-kaon fluctuations : [STAR, PRL 112, 032302 \(2014\)](#); [arXiv: 2001.02852](#); [PLB 785, 551 \(2018\)](#).



Centrality determination at lower energies



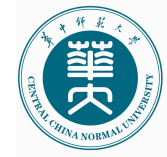
A. Chatterjee et al., arXiv:2009.03755

- At low energies, centrality resolution obtained from charge particle multiplicities is very poor and CBWC is not efficient.
- New methods, such as machine learning technique could be helpful.

F. P. Li et al., J. Phys. G 47, 115104 (2020). M. O. Kuttan et al., arXiv : 2009.01584

- Volume fluctuations corrections ?

T. Sugiura et al., Phys. Rev. C 100, (2019) 044904; Braun-Munzinger et al., Nucl. Phys. A 960 (2017)114-130
Skokov et al., Phys. Rev. C 88 (2013) 034911; HADES, PRC 102, 024914 (2020)



Efficiency Correction

Single variable and constant efficiency case.

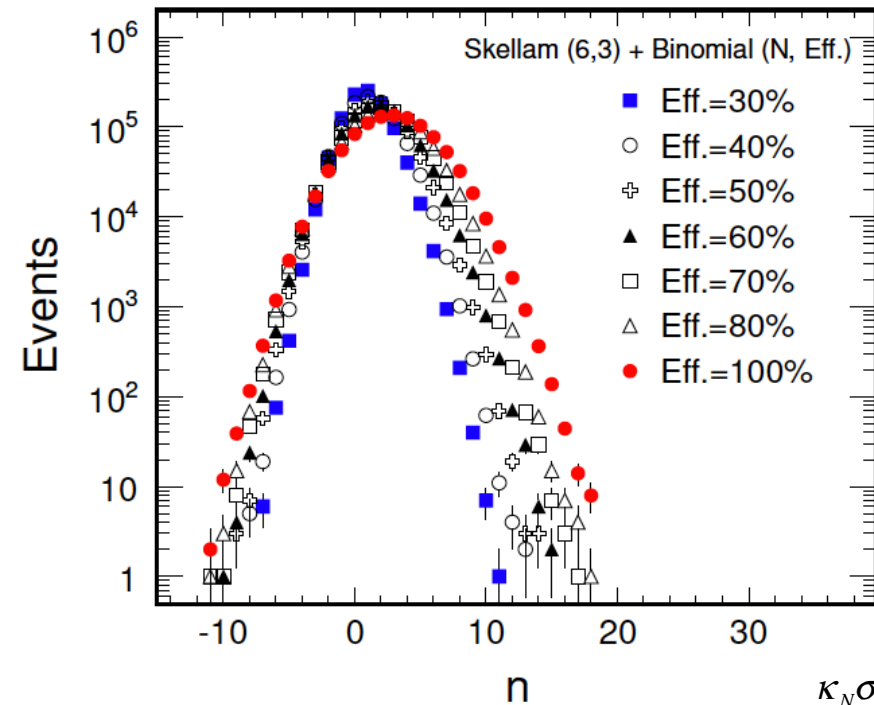
$$p(n) = \sum_N \text{Binomial}(n; N, \varepsilon) \times P(N)$$

$$B(n; N, \varepsilon) = \frac{N!}{n!(N-n)!} \varepsilon^n (1-\varepsilon)^{N-n}$$

Measure

Detector Response

Original Dis.



Mean value: $\langle N \rangle = \frac{\langle n \rangle}{\varepsilon}$

Variance: $\sigma_N^2 = \frac{\sigma_n^2 + (\varepsilon - 1) \langle n \rangle}{\varepsilon^2}$

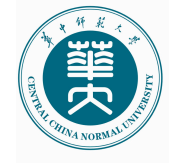
Skewness:

$$S_N \sigma_N^3 = \frac{S_n \sigma_n^3 + 3(\varepsilon - 1) \sigma_n^2 + (\varepsilon - 1)(\varepsilon - 2) \langle n \rangle}{\varepsilon^3}$$

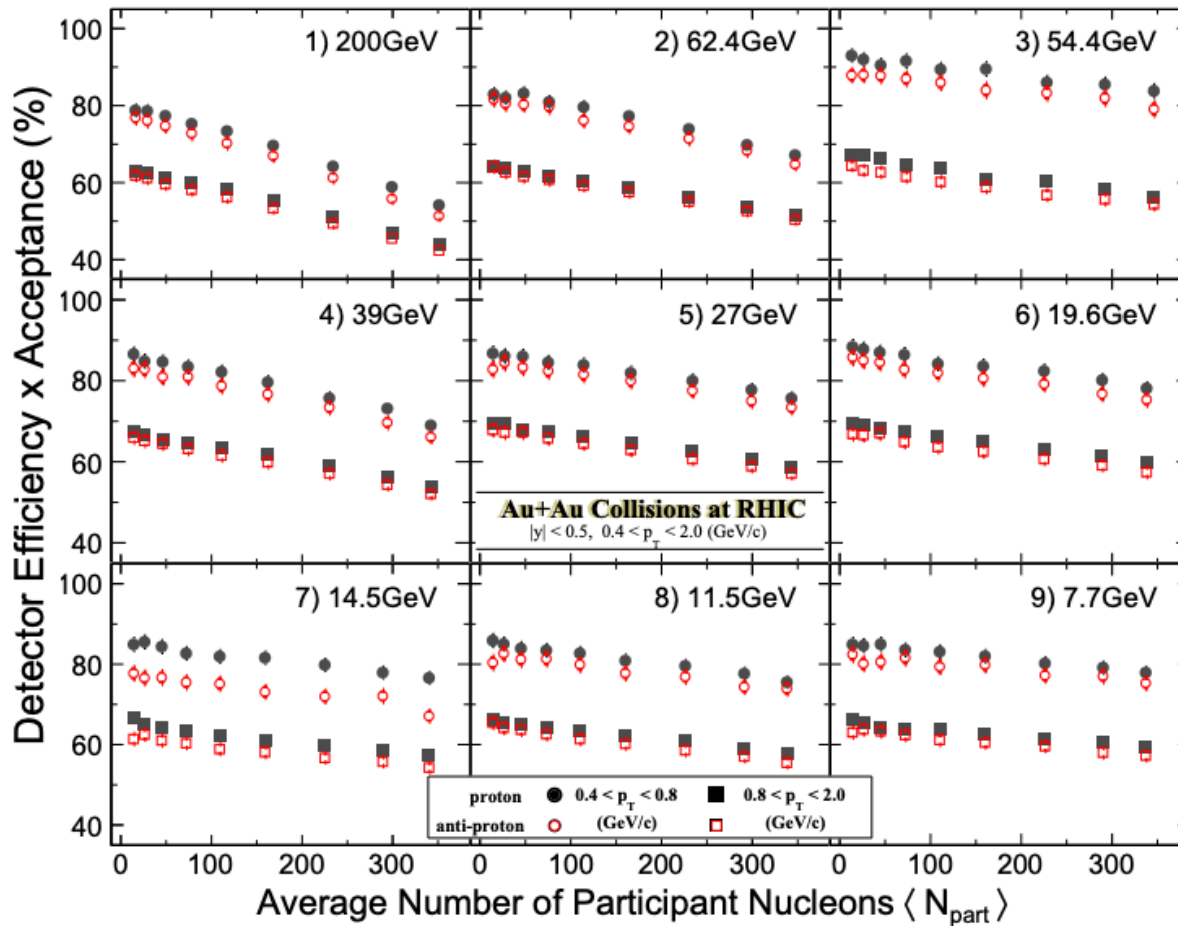
Kurtosis:

$$\kappa_N \sigma_N^4 = \frac{\kappa_n \sigma_n^4 + 6(\varepsilon - 1) S_n \sigma_n^3 + (7\varepsilon - 11)(\varepsilon - 1) \sigma_n^2 + (\varepsilon - 1)(\varepsilon^2 - 6\varepsilon + 6) \langle n \rangle}{\varepsilon^4}$$

A. Bzdak and V. Koch, PRC86, 044904 (2012)
 STAR, PRL105, 022302 (2010); PRL 112, 032302 (2014)
 X. Luo, Phys. Rev. C 91, 034907 (2015).



Efficiency for Proton and Anti-proton



low p_T (TPC PID) > High p_T (TPC+TOF PID)
Central > Peripheral
Proton > Anti-proton



Momentum Dependent Efficiency Correction

Momentum Dependent Efficiency Correction

Proton

Anti-proton

Low p_T

High p_T

Low p_T

High p_T

$$\begin{aligned}
 F_{r_1, r_2}(N_p, N_{\bar{p}}) &= F_{r_1, r_2}(N_{p_1} + N_{p_2}, N_{\bar{p}_1} + N_{\bar{p}_2}) \\
 &= \sum_{i_1=0}^{r_1} \sum_{i_2=0}^{r_2} s_1(r_1, i_1) s_1(r_2, i_2) \langle (N_{p_1} + N_{p_2})^{i_1} (N_{\bar{p}_1} + N_{\bar{p}_2})^{i_2} \rangle \\
 &= \sum_{i_1=0}^{r_1} \sum_{i_2=0}^{r_2} s_1(r_1, i_1) s_1(r_2, i_2) \langle \sum_{s=0}^{i_1} \binom{i_1}{s} N_{p_1}^{i_1-s} N_{p_2}^s \sum_{t=0}^{i_2} \binom{i_2}{t} N_{\bar{p}_1}^{i_2-t} N_{\bar{p}_2}^t \rangle \\
 &= \sum_{i_1=0}^{r_1} \sum_{i_2=0}^{r_2} \sum_{s=0}^{i_1} \sum_{t=0}^{i_2} s_1(r_1, i_1) s_1(r_2, i_2) \binom{i_1}{s} \binom{i_2}{t} \langle N_{p_1}^{i_1-s} N_{p_2}^s N_{\bar{p}_1}^{i_2-t} N_{\bar{p}_2}^t \rangle \\
 &= \sum_{i_1=0}^{r_1} \sum_{i_2=0}^{r_2} \sum_{s=0}^{i_1} \sum_{t=0}^{i_2} \sum_{u=0}^{i_1-s} \sum_{v=0}^s \sum_{j=0}^{i_2-t} \sum_{k=0}^t s_1(r_1, i_1) s_1(r_2, i_2) \binom{i_1}{s} \binom{i_2}{t} \\
 &\quad \times s_2(i_1-s, u) s_2(s, v) s_2(i_2-t, j) s_2(t, k) \times F_{u, v, j, k}(N_{p_1}, N_{p_2}, N_{\bar{p}_1}, N_{\bar{p}_2})
 \end{aligned}$$

$$F_{u, v, j, k}(N_{p_1}, N_{p_2}, N_{\bar{p}_1}, N_{\bar{p}_2}) = \frac{f_{u, v, j, k}(n_{p_1}, n_{p_2}, n_{\bar{p}_1}, n_{\bar{p}_2})}{(\varepsilon_{p_1})^u (\varepsilon_{p_2})^v (\varepsilon_{\bar{p}_1})^j (\varepsilon_{\bar{p}_2})^k}$$

Proton and anti-proton :

Low p_T : TPC

High p_T : TPC+ TOF

Factorial Moments -> Central Moments

$$\begin{aligned}
 m_n(N_p - N_{\bar{p}}) &= \langle (N_p - N_{\bar{p}})^n \rangle = \sum_{i=0}^n (-1)^i \binom{n}{i} \langle N_p^{n-i} N_{\bar{p}}^i \rangle \\
 &= \sum_{i=0}^n (-1)^i \binom{n}{i} \left[\sum_{r_1=0}^{n-i} \sum_{r_2=0}^i s_2(n-i, r_1) s_2(i, r_2) F_{r_1, r_2}(N_p, N_{\bar{p}}) \right] \\
 &= \sum_{i=0}^n \sum_{r_1=0}^{n-i} \sum_{r_2=0}^i (-1)^i \binom{n}{i} s_2(n-i, r_1) s_2(i, r_2) F_{r_1, r_2}(N_p, N_{\bar{p}})
 \end{aligned}$$

Central Moments -> Cumulant

$$C_r(N_p - N_{\bar{p}}) = m_r(N_p - N_{\bar{p}}) - \sum_{s=1}^{r-1} \binom{r-1}{s-1} C_s(N_p - N_{\bar{p}}) m_{r-s}(N_p - N_{\bar{p}})$$

A. Bzdak and V. Koch, PRC91, 027901 (2015)

X. Luo, Phys. Rev. C 91, 034907 (2015).

[Track-by-track efficiency method \(based on factorial cumulant\):](#)

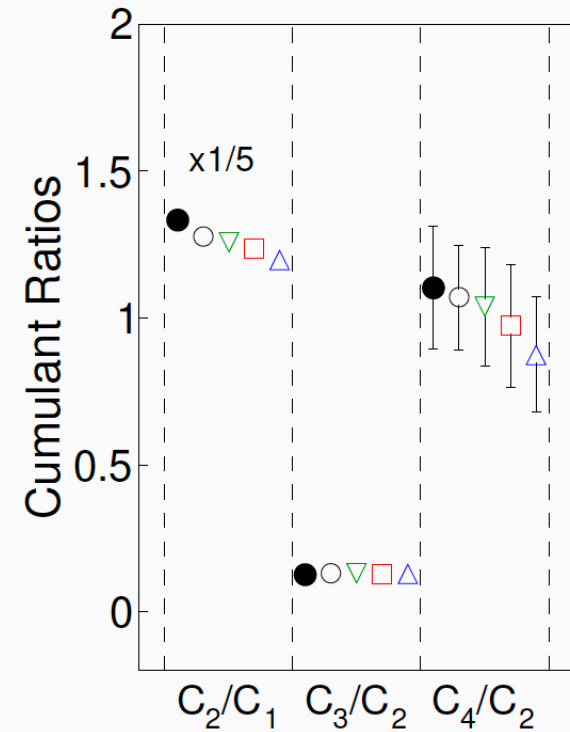
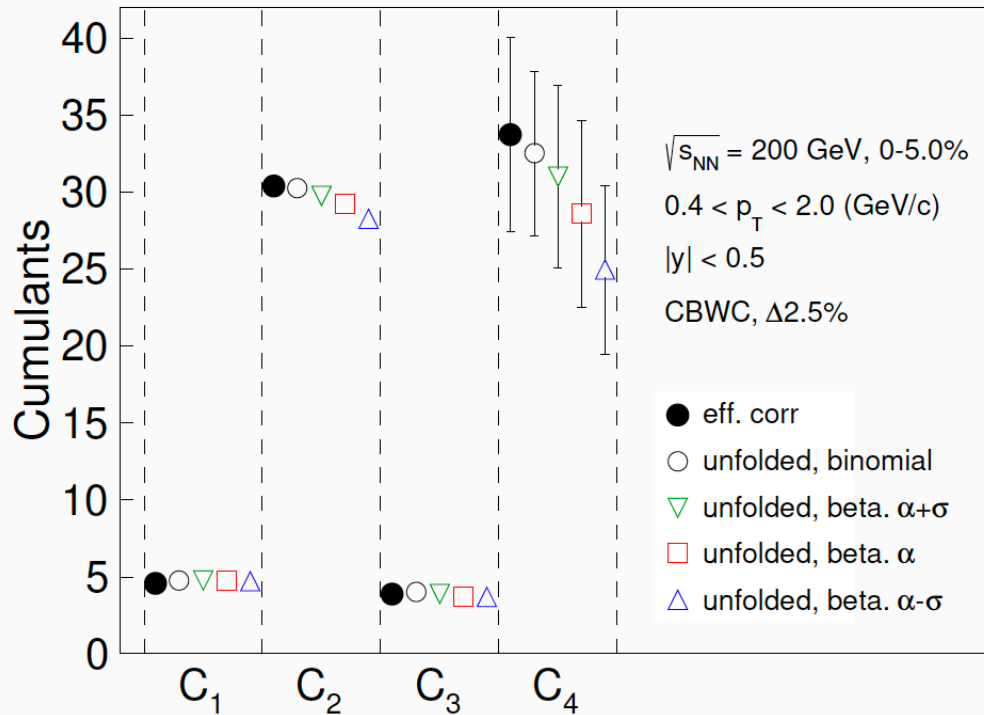
1. T. Nonaka et al., PRC95, 064912 (2017).

2. M. Kitazawa and X. Luo, PRC96, 024910 (2017).

3. X. Luo and T. Nonaka, PRC99, 044917 (2019).



Test of non-binomial effects and unfolding



STAR, arXiv: 2001.02852

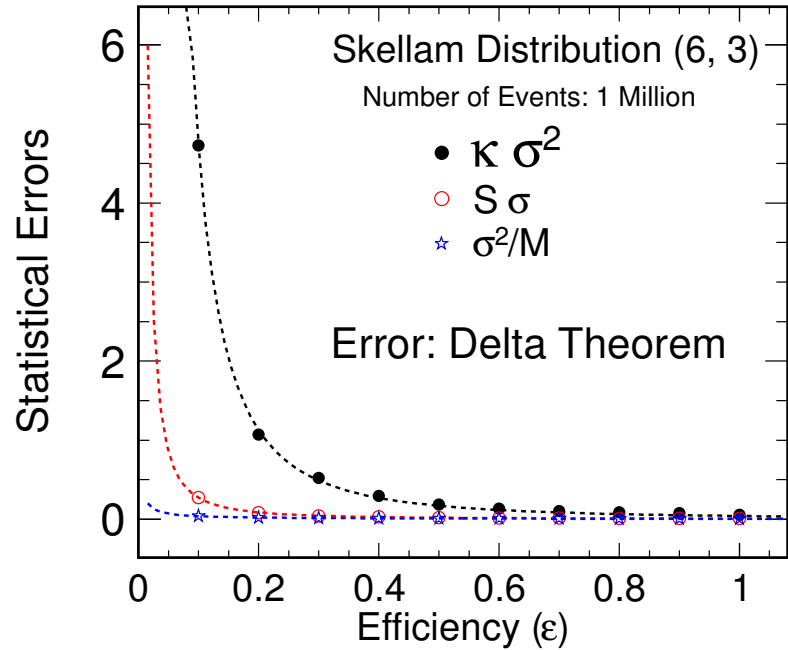
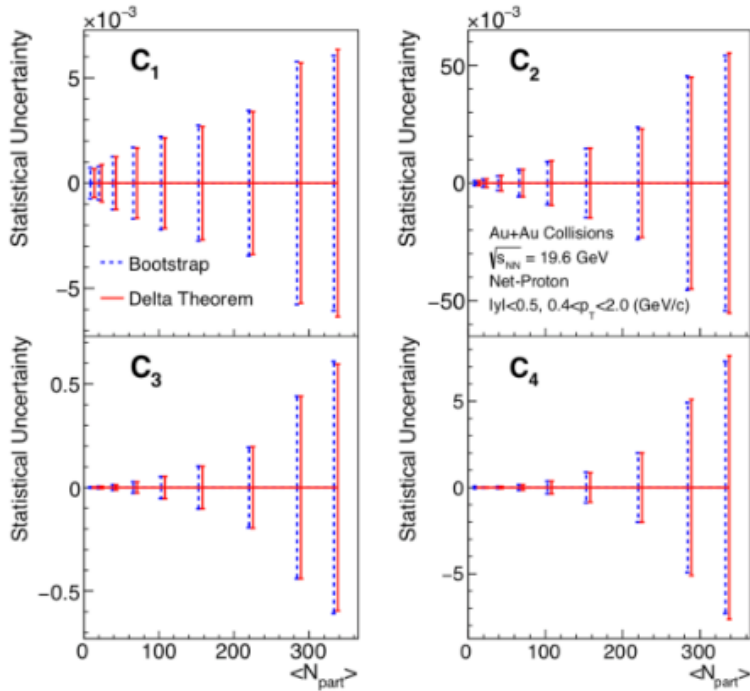
Esumi et al, arXiv:2002.11253

- The results from binomial method and unfolding method are consistent.

Conclusion : non-binomial effects are not significant for current analysis



Statistical Uncertainties in Higher Moments Analysis



Statistical errors:

- Central > Peripheral (due to width of distribution)
- Higher-order > lower order
- Delta theorem method are consistent with Bootstrap method.

$$error(\kappa\sigma^2) \propto \frac{\sigma^2}{\epsilon^2} \frac{1}{\sqrt{N_{evts}}}$$

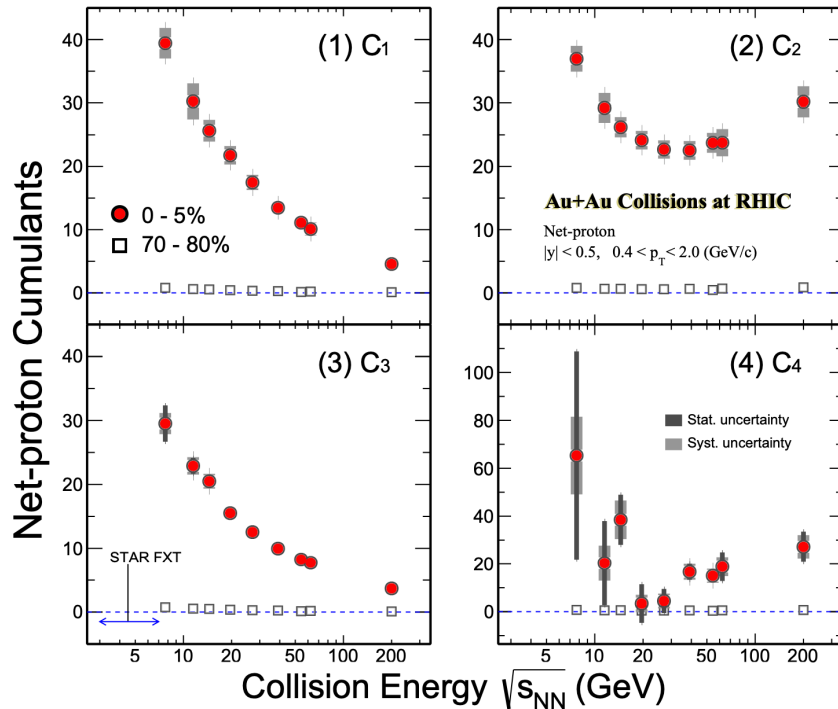
STAR : PRL 112, 032302 (2014) ; arXiv: 2001.02852.

X. Luo, J. Phys. G39, 025008 (2012); Phys. Rev. C 91, 034907 (2015);

Pandav et al, Nucl. Phys. A991, 121608 (2019)



Energy Dependence of Net-Proton Cumulant ($C_1 - C_4$)



Efficiency and CBWC corrections applied.

STAR: arXiv: 2001.02852 (short version)

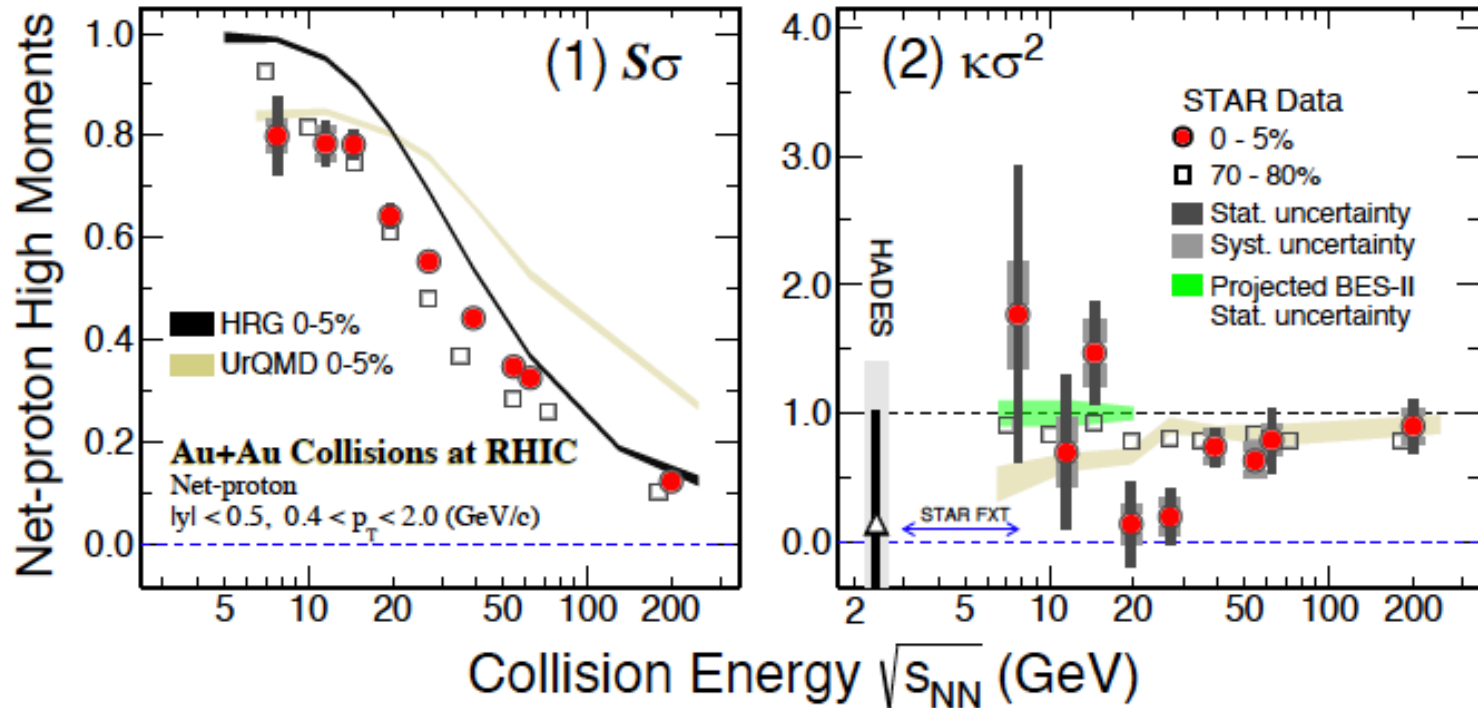
A long paper is prepared and under review process within collaboration.

- 1) Net-p, proton and anti-proton cumulants
- 2) Correlation functions of protons and anti-protons
- 3) Energy, Centrality, acceptance dependence (p_T, y).
- 4) Compare the data with various model results .

- Cumulants of net-proton distributions from 0-5% central and 70-80% peripheral collisions.
- Mean values increase when energy decreases due to baryon stopping.
- Cumulants can be decomposed into various order correlation functions, which will provide additional information for underlying physics.



Energy Dependence of Cumulant Ratios : $S\sigma$ and $\kappa\sigma^2$



- HRG (GCE) and transport model predicted monotonical energy dependence. Suppression at low energy due to conservation.
- Observe a non-monotonic energy dependence (7.7-62.4 GeV) in 0-5% net-proton $\kappa\sigma^2$ with a significant of 3.1σ

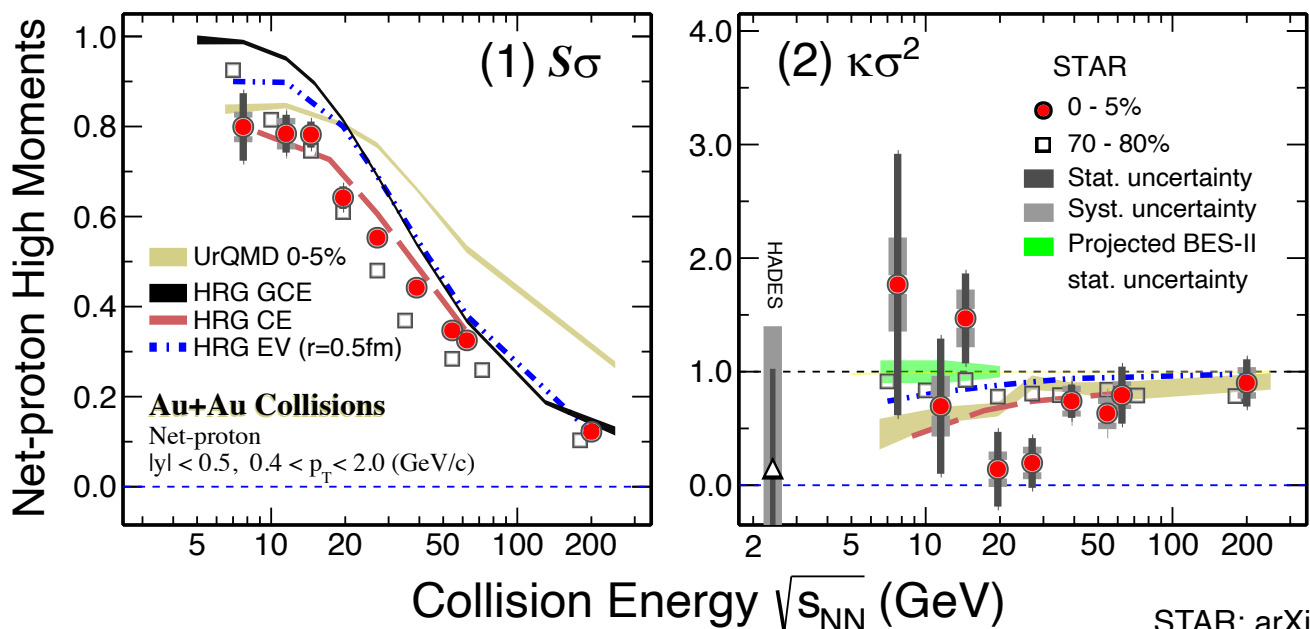
HADES, PRC 102, 024914 (2020)
STAR, arXiv: 2001.02852

Is there a peak structure below 20 GeV ?

Need precise measurement at STAR (BES-II), CBM, NICA etc.



Comparison between model calculations and exp. data



- PBM et al. proposed the Canonical Ensemble (CE) for describing the system at high baryon density (baryon number conservation). Their calculations are consistent with transport model results.
- Excluded volume (EV) approach also leads to suppression at high baryon region.
'repulsive force' suppress the fluctuations. 'Attractive' of protons at the 7.7 GeV collisions ?
- Goodness of the description between data and model results are evaluated with the p values obtained from χ^2 test.

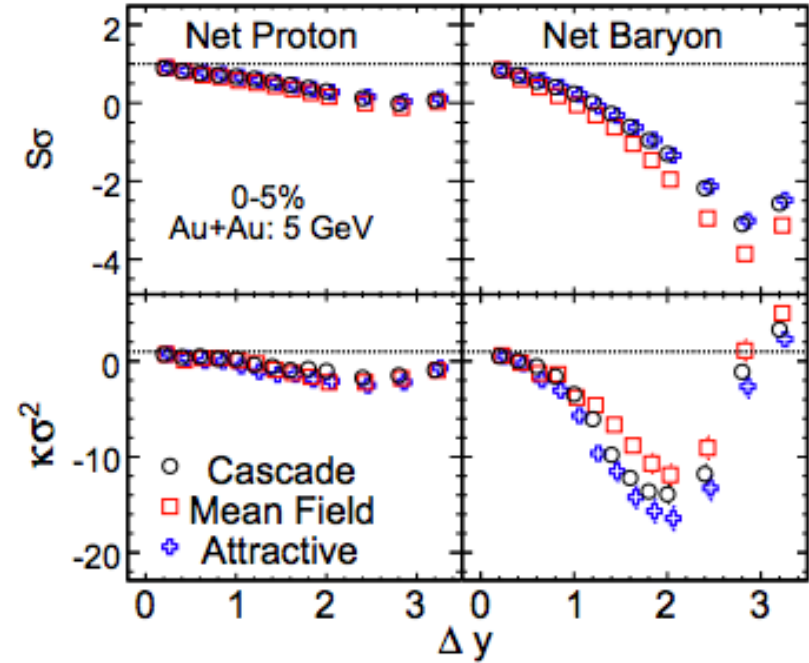
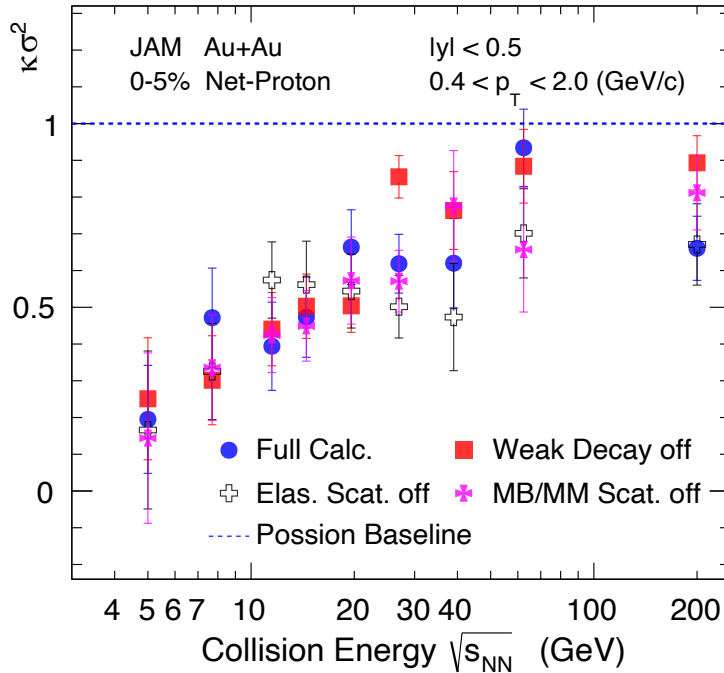
p values from χ^2 test below 27 GeV

PBM et al., arXiv: 2007.02463, S. He et al., PLB 762 296 (2016).
 J.H. Fu, PLB 722, 144 (2013), A. Bhattacharyya et al., PRC 90, 034909(2014).
 HRG+VDW: Vovchenko et al., PRC92,054901 (2015); PRL118,182301 (2017).
 RMF: K. Fukushima, PRC91 044910 (2015)

Moments	HRG GCE	HRG EV ($r = 0.5 \text{ fm}$)	HRG CE	UrQMD
$S\sigma$	< 0.001	< 0.001	0.0754	< 0.001
$\kappa\sigma^2$	0.00553	0.0450	0.0145	0.0221



Non-critical contributions: transport model studies



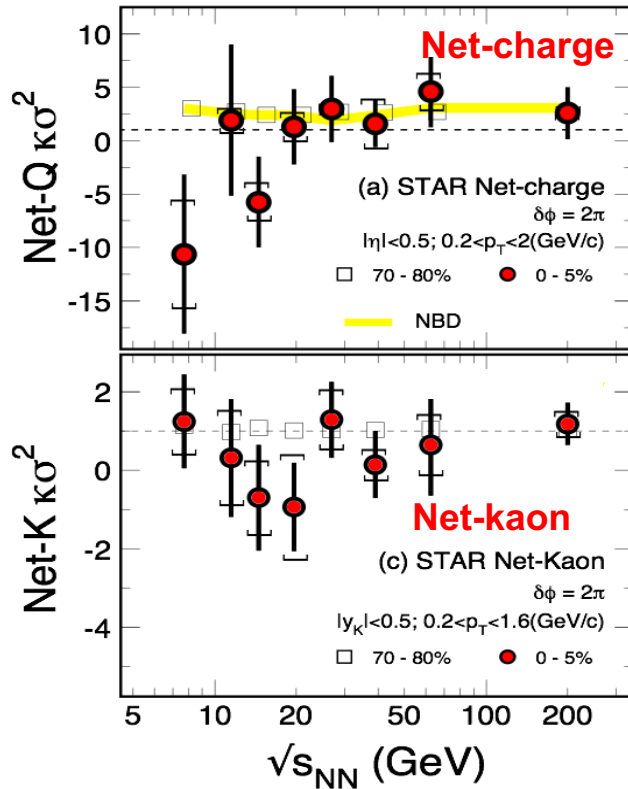
UrQMD, JAM, AMPT : Dominated by baryon number conservations at low energies

- Effects of weak decay and hadronic scattering are not significant within uncertainties.
- No significant effects observed for mean field potential and attractive scattering (to simulate softening of EoS)

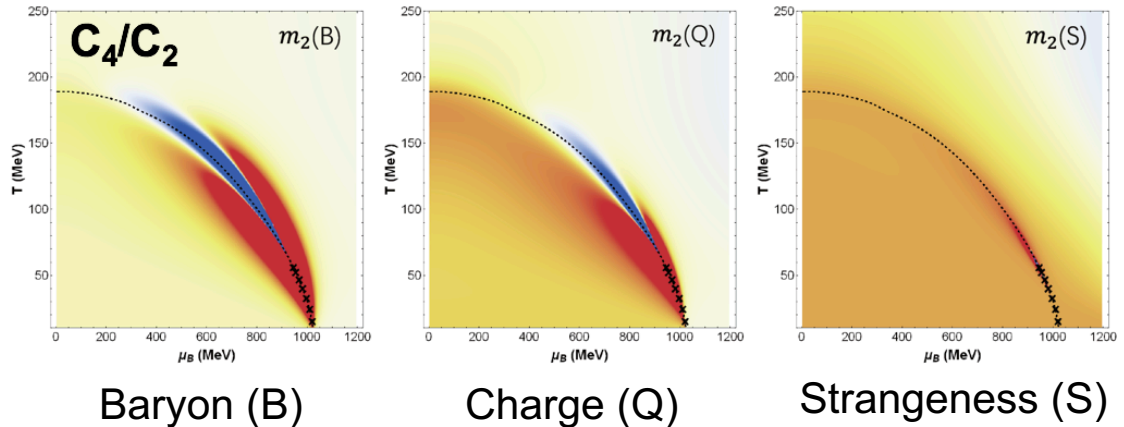
Z. Feckova, et al., PRC92, 064908(2015); J. Xu, et. al., PRC94, 024901(2016); X. Luo et al., NPA931, 808(14), P.K. Netrakanti et al., NPA947, 248(2016), P. Garg et al. PLB 726, 691(2013). S. He, et. al., PLB762, 296 (2016); PLB 774, 623 (2017). J. Li et al, PRC 97,014902 (2018). H. J. Xu, PLB 765, 188 (2017); Y. X. Ye et al., PRC 98, 054620 (2018). C. Zhou, et al., PRC 96, 014909 (2017). Y. Zhang, et al. PRC101, 034909 (2020). L. Jiang et al., PRC94, 024918 (2016); M. Bluhm, EPJC77, 210 (2017).

Net-charge and Net-kaon Fluctuations

STAR Data



NJL Model calculations



W. Fan, X. Luo, H.S. Zong, IJMPA 32, 1750061 (2017).

Critical signals: B>Q>S

(Due to the mass of strange quark is much larger than u,d quarks, $m_s \gg m_{u,d}$)

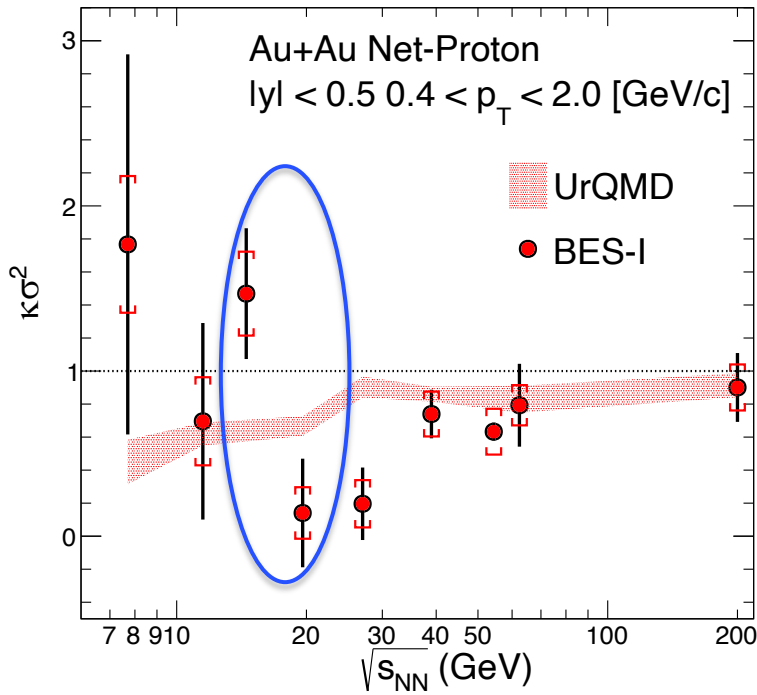
$$error(\kappa\sigma^2) \propto \frac{\sigma^2}{\epsilon^2} \frac{1}{\sqrt{N_{evts}}}$$

STAR : Phys. Rev. Lett. 113 092301 (2014).
 Phys. Lett. B 785, 551 (2018).

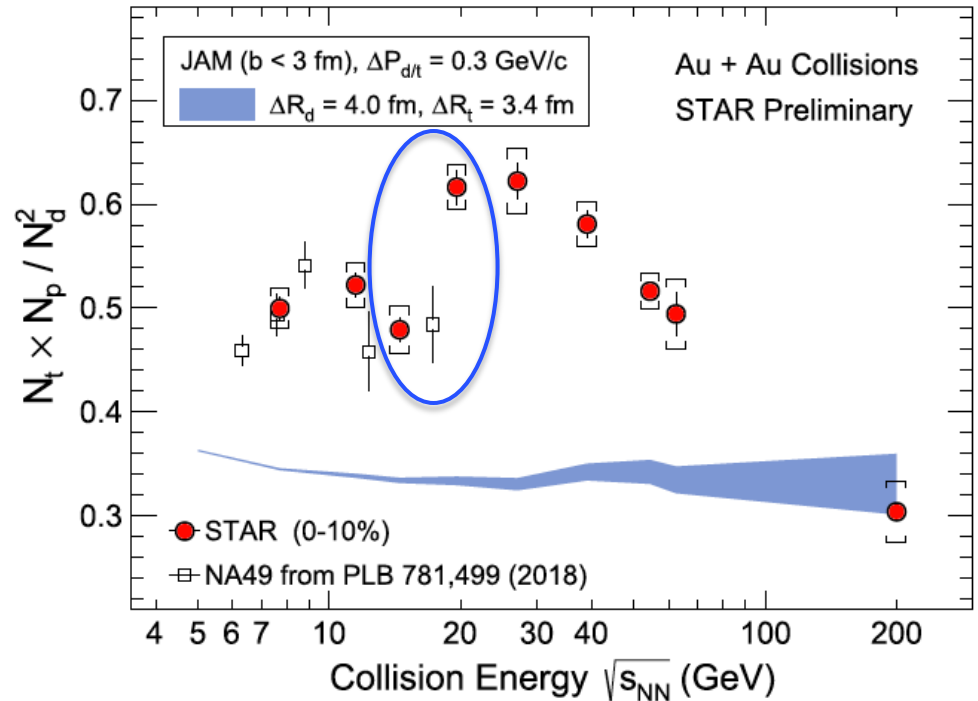
- 1) Within errors, the results of net-Q and net-Kaon show flat energy dependence.
- 2) More statistics are needed, especially at low energies (BES-II will help).



Propose to take the data of Au+Au collisions at 17.1 GeV



STAR: arXiv: 2001.02852



Dingwei Zhang (STAR), QM2019 [arXiv: 2002.10677]

1. Value jumps between 19.6 and 14.5 GeV in both net-proton flu. and light nuclei yield ratio.
2. STAR has proposed to take a new energy point in 2021 (Run 21) : **17.1 GeV** ($\mu_B \sim 235$ MeV) with μ_B lie between 14.5 ($\mu_B \sim 266$ MeV) and 19.6 GeV ($\mu_B \sim 205$ MeV).

Model calculations trying to explain both observations :

Pre-cluster at chemical freeze-out due to attractive NN potential :

2.5 Weeks with ~250 million events.

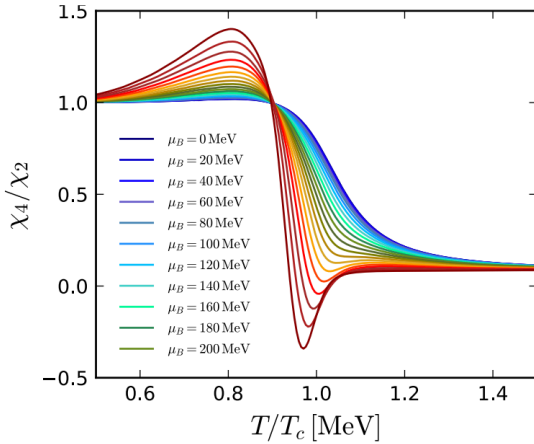
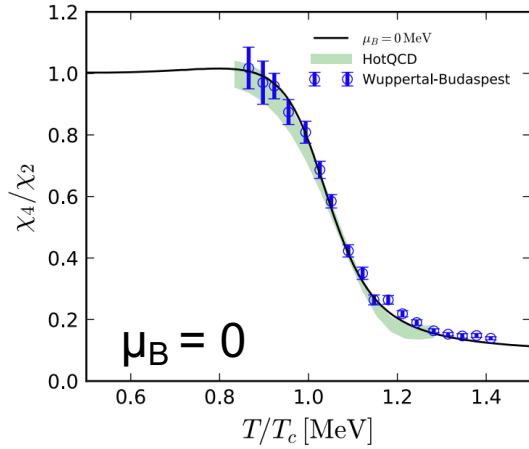
Edward Shuryak, Juan M. Torres-Rincon, PRC 100, 024903 (2019);

PRC 101, 034914 (2020); EPJA 56, 241 (2020).

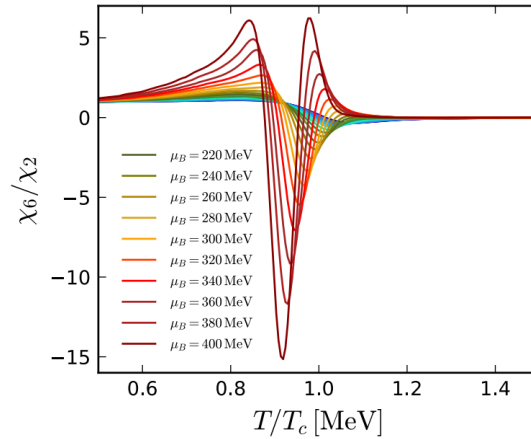
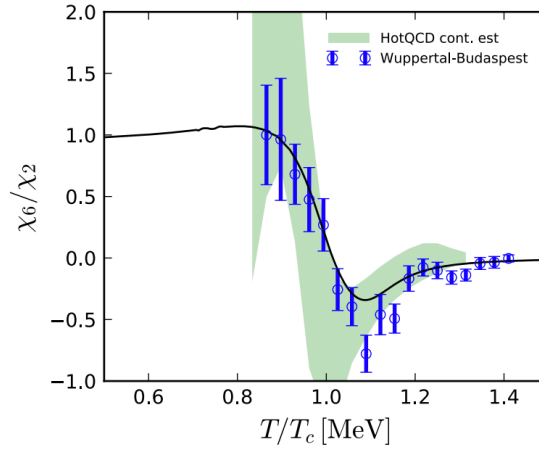


Higher-order baryon number fluctuations: PQM+FRG Model

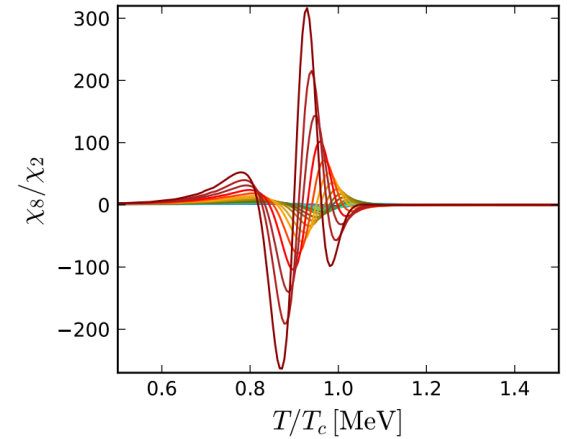
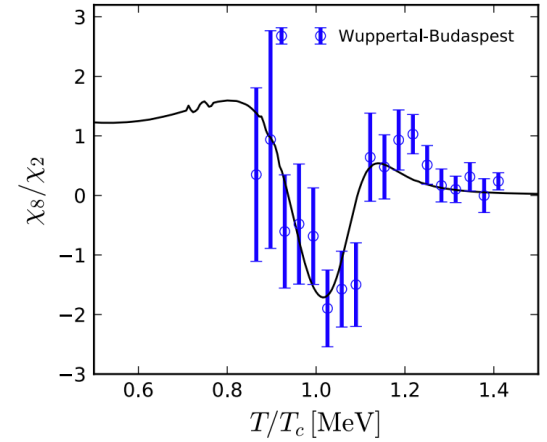
4th order



6th order

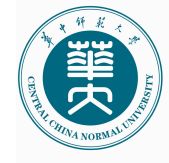


8th order

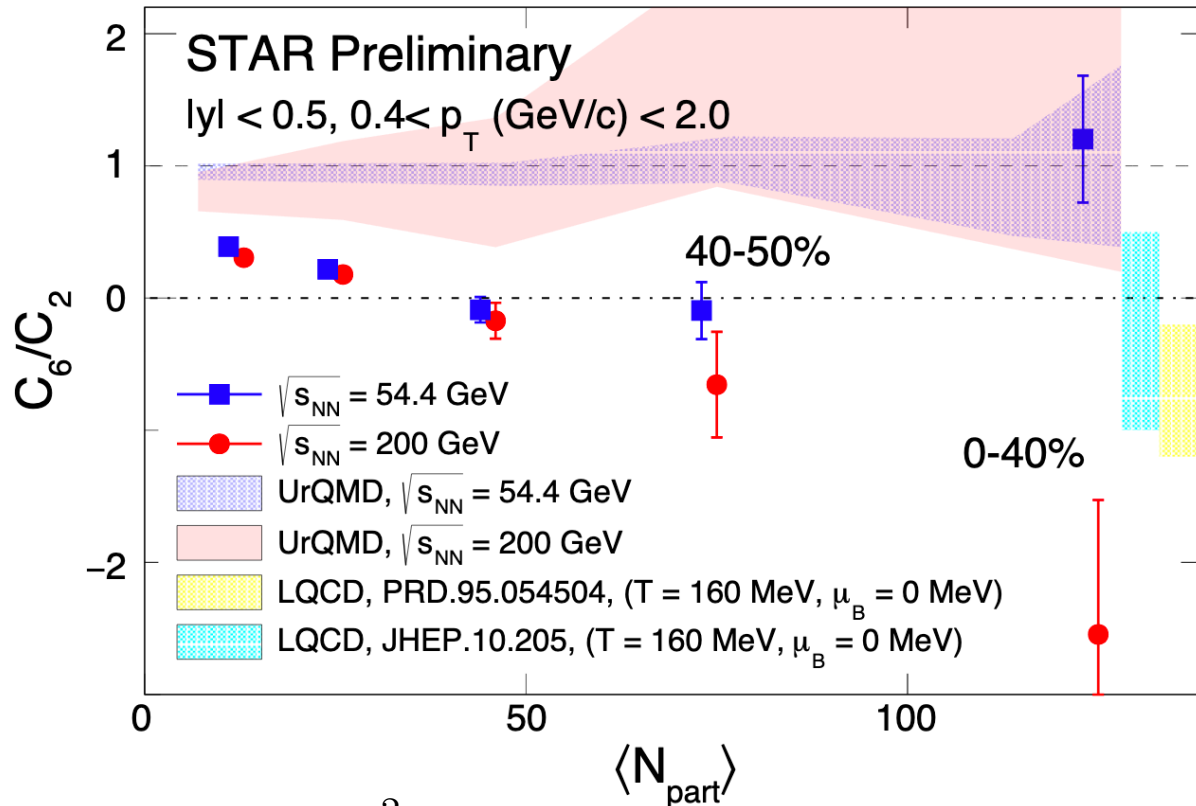


- Higher-order fluctuations are more sensitive to QCD phase transition.
 - At $\mu_B = 0$, $C_6 \sim 0$ or negative, and C_8 become negative when chemical freeze-out temperature close to T_c .
- > could serve as experimental evidence of chiral crossover.

Wei-jie Fu et al., In preparation.



Net-proton C_6 measurement



$$\text{error}(C_n/C_2) \propto \frac{\sigma^{n-2}}{\sqrt{N}\epsilon^\alpha}$$

Ashish and Toshihiro, QM2019

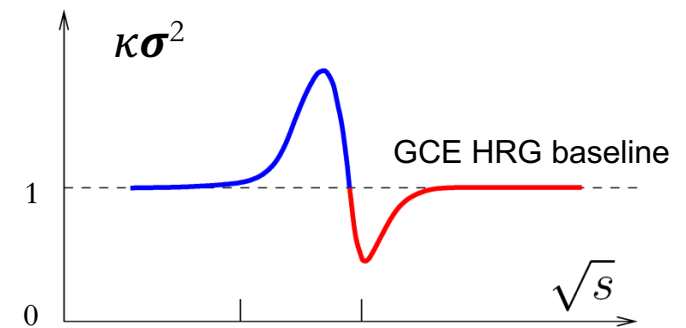
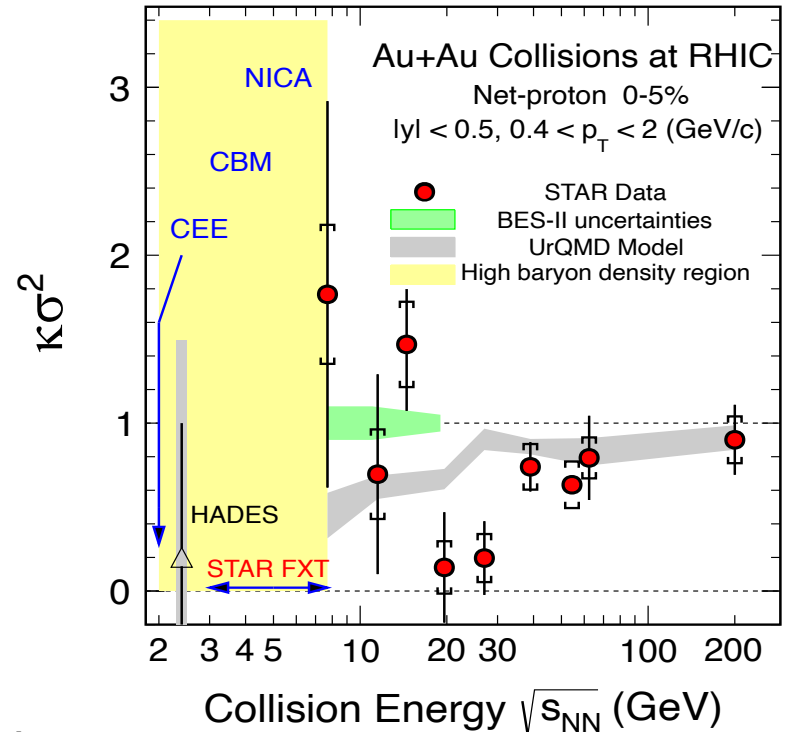
- Results from three energies are consistent in peripheral collisions.
- $C_6/C_2 > 0$ at 54.4 GeV and $C_6/C_2 < 0$ at 200 GeV in 0-40% central collisions.



BES-II at RHIC (2019-2021)

$\sqrt{s_{NN}}$ (GeV)	Events (10^6)	BES II / BES I
19.6	538	2019 / 2011
14.6	325	2019 / 2014
11.5	230	2020 / 2010
9.2	160	2020 / 2008
7.7	100	2021 / 2010
17.1	250	2021 (proposed)

STAR, arXiv: 2001.02852



- BES-II: 10-20 times higher statistics than BES-I.
- FIX-target mode : $\sqrt{s_{NN}} = 3-7.7$ GeV (2018-2021).

iTPC, ETOF, EPD upgrade completed.

- Enlarge Acceptance : η coverage from 1.0 to 1.5
- Improve dE/dx and forward PID
- Improve centrality/event plane determination



BES-I & II at RHIC (2010-2017, 2019-2021)

Collider mode

Au+Au Collisions

FXT mode

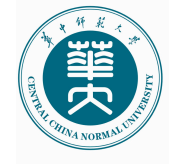
$\sqrt{s_{NN}}$ (GeV)	Events (10^6)	BES II / BES I	μ_B (MeV)	T_{CH} (MeV)
200	238	2010	25	166
62.4	46	2010	73	165
54.4	1200	2017	83	165
39	86	2010	112	164
27	30 (560)	2011/2018	156	162
19.6	538 / 15	2019/2011	206	160
14.5	325 / 13	2019/2014	264	156
11.5	230 / 7	2020/2010	315	152
9.2	160 / 0.3	2020/2008	355	140
7.7	100 / 3	2021/2010	420	140
17.1*	250	2021	230	158

$\sqrt{s_{NN}}$ (GeV)	Events (10^6)	BES II / BES I	μ_B (MeV)	T_{CH} (MeV)
7.7	50+112	2019+2020	420	140
6.2	118	2020	487	130
5.2	103	2020	541	121
4.5	108	2020	589	112
3.9	117	2020	633	102
3.5	116	2020	666	93
3.2	200	2019	699	86
3.0	259	2018	720	80
3.0*	2000	2021	720	80

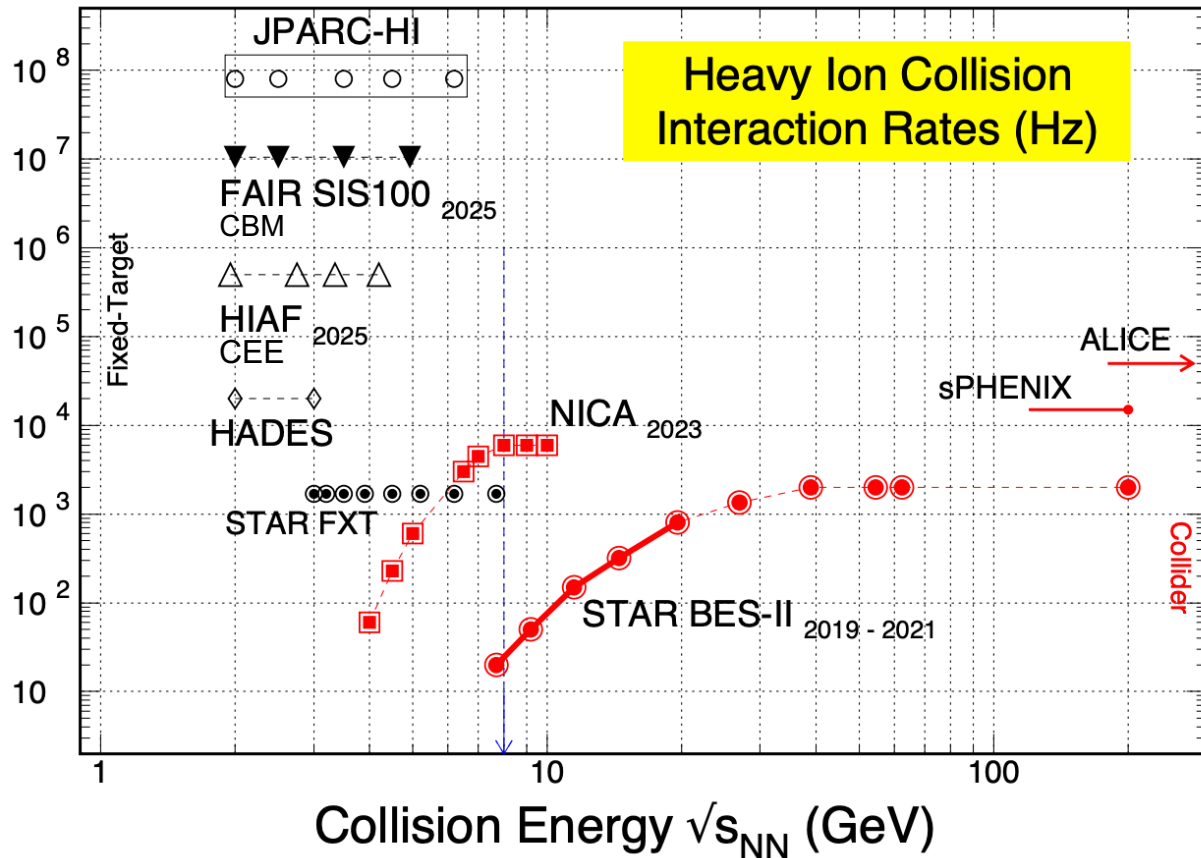
T_{ch} and μ_B from J. Cleymans et al. PRC73, 034905 (2006)
 *New Proposed Energy in Beam User Request 2020/2021.

BES-II Program:

- Precisely map the QCD phase diagram $200 < \mu_B < 420$ MeV
- The FXT program extends μ_B coverage up to 720 MeV (3 GeV)



Future Facilities for Heavy-Ion Collisions



X. Luo, N. Xu, Nucl. Sci. Tech. 28, 112 (2017).

X. Luo, S. Shi, N. Xu and Y. Zhang, Particle 3, 278 (2020)

A. Bzdak, S. Esumi, V. Koch, J. Liao, M. Stephanov, N. Xu Phys. Rep. 853, 1 (2020).

K. Fukushima, B. Mohanty, N. Xu, arXiv: 2009. 03006

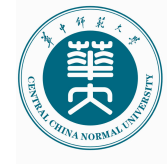
Exploring the QCD phase structure at high baryon density region



Summary and Outlook

Higher moments of conserved quantities and light nuclei production are sensitive observables of CP (large density fluctuations and long range correlations)

- Yield ratio of light nuclei and fourth order net-proton fluctuations (C_4/C_2) in central Au+Au collisions shows non-monotonic energy dependence, which could serve as important experimental basis for critical point search.
- Hypernuclei production is important to study Y-N interactions and probe baryon-strangeness correlations, which can be enhanced near CP or 1st order P. T.
- C_6 and C_8 can be used to probe the chiral crossover at $\mu_B=0$. Large statistics are needed to conduct precise measurements.
- Need to study the background/non-equilibrium contributions carefully and build-up dynamical modeling of heavy-ion collisions with critical fluctuations.
- Explore the QCD phase structure at **high baryon density** with **high precision**:
 - (1) RHIC BES-II : Collider ($\sqrt{s_{NN}} = 7.7 - 19.6$ GeV) and FXT ($\sqrt{s_{NN}} = 3 - 7.7$ GeV) mode.
 - (2) Future Facilities ($\sqrt{s_{NN}} = 2 - 11$ GeV) : FAIR/CBM, NICA/MPD, HIAF/CEE, JPARC-HI.



Acknowledgements :

Thanks to the members of the STAR Collaboration and the kind invitation from the organizers.

Thank you for your attention !

Stay safe and take care